



# Unveiling hidden threats: Nitrate pollution in agricultural catchments with deep vadose zone



Min Ren <sup>a,b</sup>, Xining Zhao <sup>c,d</sup>, Ruxin Shao <sup>a,b</sup>, Mingyi Wen <sup>c,d</sup>, Xiaodong Gao <sup>c,d</sup>, Liuyang Yu <sup>c,d</sup>, Nanfang Ma <sup>a,b</sup>, Ting Yang <sup>e</sup>, Jingdan Zhao <sup>f</sup>, Changjian Li <sup>c,d,\*</sup>

<sup>a</sup> Key Laboratory of Agricultural Soil and Water Engineering in Arid and Semiarid Areas, Ministry of Education, Northwest A&F University, Yangling, Shaanxi Province 712100, China

<sup>b</sup> College of Water Resources and Architectural Engineering, Northwest A&F University, Yangling, Shaanxi Province 712100, China

<sup>c</sup> Institute of Soil and Water Conservation, Northwest A&F University, Yangling, Shaanxi Province 712100, China

<sup>d</sup> Institute of Soil and Water Conservation, Chinese Academy of Science & Ministry of Water Resources, Yangling, Shaanxi Province 712100, China

<sup>e</sup> Shaanxi Agricultural Radio and Television School Changwu Branch, Xianyang, Shaanxi Province 713600, China

<sup>f</sup> Inner Mongolia Autonomous Region Farmland Construction Service Center, Hohhot, Inner Mongolia Autonomous Region 010010, China

## ARTICLE INFO

### Keywords:

Non-point source pollution  
Nitrogen balance  
Nitrate source  
Heavy precipitation  
Hydrological process

## ABSTRACT

Identifying dominant nitrogen sources in groundwater and surface water is critical for controlling non-point source (NPS) pollution in agricultural watersheds. However, in regions with deep vadose zones ( $>4$  m) and limited precipitation. However, in regions with deep vadose zones ( $>4$  m) and limited precipitation, the hidden threats of agricultural NPS pollution remain critically understudied due to prolonged pollution retention and insufficient transport dynamics. Here, we investigated the transport routes of surplus N and the driving mechanism of NPS pollution in a semi-humid agricultural catchment with vadose zone thickness exceeding 80 m and large-scale apple orchards, through a combined approach of questionnaire survey, hydrochemistry, multi-isotope tracer technology ( $\delta^{15}\text{N-NO}_3$ ,  $\delta^{18}\text{O-NO}_3$ ,  $\delta^2\text{H-H}_2\text{O}$ ,  $\delta^{18}\text{O-H}_2\text{O}$ ) and MixSIAR model. The results indicated that the high nitrogen input and surplus in apple orchards led to an annual potential nitrogen loss in runoff up to  $257.88 \text{ kg-ha}^{-1}$ , 3.7 times that of croplands. Heavy precipitation was the main driving force for the loss of residual soil nitrogen. As the main form of inorganic nitrogen in water, the nitrate concentration in surface water peaked at  $8.63 \text{ mg L}^{-1}$  during heavy rainfall, approaching the drinking water safety threshold of World Health Organization. Simultaneously, precipitation contribution to surface water increased sharply to 66.2 %. This resulted in a rapid rise in the proportion of nitrate derived from fertilizer and soil nitrogen, rising from 2 % to 90 %. Thus, the surface water nitrate mainly originated from agricultural surplus nitrate during heavy precipitation. In contrast, during periods without heavy precipitation, groundwater was the dominant source ( $>80$  %) of surface water recharge, making groundwater the main source of surface water nitrate. Critically, the deep vadose zone has effectively impeded the leaching of agricultural surplus nitrate into groundwater so far. Therefore, groundwater nitrate and surface water nitrate without heavy precipitation both mainly ( $> 90$  %) originated from manure and sewage. This study emphasized that heavy precipitation periods were the high-risk intervals for nitrogen NPS pollution in agricultural area with deep vadose zone and limited precipitation, providing scientific support for targeted NPS pollution prevention and control strategies.

## 1. Introduction

Nitrogen (N) pollution has emerged as a global environmental concern because it could lead to eutrophication and hypoxia, water quality damage, health degradation of aquatic ecosystems, which seriously threatens water security and restricts regional sustainable

development (Zhang et al., 2021b; Schulte-Uebbing et al., 2022; Dodds and Smith, 2016; Xiao et al., 2020; Qin et al., 2023). N pollution of non-point source (NPS) is particularly challenging to control due to its dispersed sources, unpredictable release, and delayed impact (An et al., 2023; Xiao et al., 2019). The main causes of agricultural NPS pollution are the excessive use of chemical fertilizer caused by intensive

\* Correspondence to: Institute of Soil and Water Conservation, Northwest A&F University, No.26 Xinong Road, Yangling, Shaanxi Province 712100, China.  
E-mail address: [lichangjian@nwafu.edu.cn](mailto:lichangjian@nwafu.edu.cn) (C. Li).

agricultural development, and the unreasonable discharge of domestic sewage and livestock and poultry manure (Ongley et al., 2010). Especially in regions with fragile ecosystems or significant conflicts between population and agricultural lands, the formation mechanisms of agricultural NPS pollution exhibit greater complexity and are influenced by multiple factors (Liu et al., 2018; Kataoka et al., 2019; Zou et al., 2020; Wang et al., 2025).

Key factors determining the pollution degree include the intensity of pollution source, vadose zone thickness, soil texture, precipitation or irrigation intensity, vegetation type, and land use type (Zhang et al., 2021b; El Mountassir et al., 2022). Numerous studies have explored the source and transport of nitrate ion ( $\text{NO}_3^-$ ) in areas with abundant precipitation or adequate irrigation (Fuentes-Rivas et al., 2020; Mo et al., 2022), thin soil layers, shallow groundwater level (Libutti and Monteleone, 2017; Serra et al., 2021), and where N pollution has significantly impacted local groundwater and surface water (Hou et al., 2023). However, N pollution of NPS in agricultural areas with deep vadose zones ( $> 4 \text{ m}$ ) or limited precipitation has often been neglected due to the delayed impact of groundwater N pollution and the increased uncertainty of surface water N pollution (He et al., 2020, 2024; Wang et al., 2023). Through monitoring water quality in 175 wells in an intensive apple-growing region of the southern Loess Plateau, China, Zhu et al. (2023) revealed that the average groundwater  $\text{NO}_3^-$  concentrations in rainfed areas, well-irrigated areas, and canal-irrigated areas were 9, 23, and  $94 \text{ mg L}^{-1}$ , respectively. Additionally,  $\text{NO}_3^-$  concentrations in wells with water table depths of 8 m, 10 m, and 12 m were 208, 68, and  $55 \text{ mg L}^{-1}$ , respectively. Mihiranga et al. (2022) explored the mechanism of N export control in a semi-arid mountains watershed in North China and proved that  $\text{NO}_3^-$ -N contributed 69.6 % of TN, and storm runoff increased the N flux by 3–4 times on average. Although there have been some studies on water nitrate pollution in regions with limited precipitation and deep vadose zones (Broxton and Vaniman, 2005; Zhang et al., 2013; Miao et al., 2023), the extent to which nitrogen surplus in rain-fed agricultural areas affect groundwater and surface water nitrate remains unclear, particularly regarding quantitative seasonal  $\text{NO}_3^-$  source apportionment. Therefore, after clarifying N surplus from major crops, identifying the  $\text{NO}_3^-$  sources in groundwater and surface water becomes necessary for exploring NPS pollution in rainfed agricultural areas with deep vadose zone and limited precipitation.

Among various methods for differentiating  $\text{NO}_3^-$  sources (Samantara et al., 2015; He and Lu, 2016; Shukla and Saxena, 2020), the dual nitrate stable isotope ( $\delta^{15}\text{N}-\text{NO}_3/\delta^{18}\text{O}-\text{NO}_3$ ) approach serves as one of the most efficient tools since each  $\text{NO}_3^-$  source typically exhibits a unique isotopic signature (Ren et al., 2022). Sources of  $\text{NO}_3^-$  mainly include atmospheric deposition (DN), chemical fertilizer (FN), manure and sewage (MN) and soil N (SN). The challenge in accurately identifying nitrate sources arises from signal overlaps among different sources and the interference of nitrification and denitrification processes (Xue et al., 2009). To address this, several studies have combined the dual nitrate stable isotope with hydrochemistry, other stable isotopes (e.g.,  $\delta^{34}\text{S}-\text{SO}_4$ ,  $\delta^{87}\text{Sr}/\delta^{86}\text{Sr}$ ,  $\delta^{11}\text{B}$ ,  $\delta^{13}\text{C}-\text{DIC}$ ) (Torres-Martínez et al., 2020; Ren et al., 2022; Kaown et al., 2023a), noble gases, metabolic genes (Ju et al., 2023), land use (Gao et al., 2021a), and Bayesian models (SIAR, SIR, and MixSIAR) (Wang et al., 2023) to achieve a more accurate analysis of nitrate sources.

Water flow is the main carrier of N transport, the hydrological cycle profoundly influences the migration path of  $\text{NO}_3^-$  (Kaown et al., 2023b). Therefore, it is crucial to clarify the water cycle characteristics and the conversion relationship between groundwater and surface water to explore the driving mechanism of NPS pollution of N. As the smallest natural water collection unit and the primary source of NPS pollution, headwater catchments play crucial roles in providing drinking water, irrigation, flood drainage and downstream water sources in agricultural areas (Xu et al., 2018). However, in rain-fed agricultural areas with limited precipitation and deep vadose zones, the response mechanism of  $\text{NO}_3^-$  sources in surface water to different recharge conditions remains unclear. In previous studies, hydrological series analysis (Juez et al.,

2022), hydrological models (Zhai et al., 2021) and digital filter (Lyu et al., 2022) were commonly used to explore the water cycle of watersheds, but they were not suitable for catchments lacking long-term series hydrological monitoring data (Fatichi et al., 2016). The application of  $\delta^2\text{H}-\text{H}_2\text{O}$  and  $\delta^{18}\text{O}-\text{H}_2\text{O}$  offers a good alternative to segment base flow (Li et al., 2023), making the combination with  $\delta^{15}\text{N}-\text{NO}_3$ ,  $\delta^{18}\text{O}-\text{NO}_3$  isotopes an effective method for accurately tracing  $\text{NO}_3^-$  and exploring the NPS pollution mechanism in catchment lacking long-term monitoring hydrological data.

Based on previous studies, we put forward following hypothesis: although deep vadose zones and limited precipitation reduced the speed and intensity of N release to water, agricultural excess N still entered groundwater and surface water. To verify the hypotheses, we selected Wangdonggou catchment, a typical rain-fed agricultural headwater catchment with vadose zone and limited precipitation in the south of Loess Plateau of China, as the study area. The catchment is the most typical region within Loess Plateau in terms of climate, topography, crop types, livestock types, and agricultural population density. We explored the mechanism of N pollution of NPS in a rain-fed agricultural catchment with deep vadose zone and limited precipitation, combining multiple isotopes ( $\delta^{15}\text{N}-\text{NO}_3$ ,  $\delta^{18}\text{O}-\text{NO}_3$ ,  $\delta^2\text{H}-\text{H}_2\text{O}$ ,  $\delta^{18}\text{O}-\text{H}_2\text{O}$ ), hydrochemistry data ( $\text{NO}_3^-$ ,  $\text{NH}_4^+$ , TN,  $\text{Cl}^-$ ) and MixSIAR model, after collecting groundwater, surface water and precipitation samples in the headwater catchment for 2 years. The main objectives of this study were as follows: (1) estimate the N balance of main crops in the catchment; (2) explore the effects of N surplus on N occurrence and nitrate sources in groundwater and surface water; (3) explore the driving mechanism of NPS pollution of N under different seasons and precipitation conditions. The results could contribute to the further understanding of the source and fate of N in agricultural areas characterized by semi-arid or semi-humid deep vadose zones.

## 2. Materials and methods

### 2.1. Study area

Wangdonggou catchment ( $35^\circ 12' \sim 35^\circ 16'\text{N}$ ,  $107^\circ 40' \sim 107^\circ 42'\text{E}$ ) covers an area of  $8.3 \text{ km}^2$  and belongs to the semi-humid zone with an average annual precipitation of 584 mm. The depth of the vadose zone in more than half of the catchment areas is more than 80 m. It is dry in winter and spring and rainy in summer and autumn. The average monthly precipitation from 1998 to 2023 is shown in Fig.S1. The Loess Plateau, to which the catchment belongs, is a typical rain-fed agricultural region characterized by a fragile ecological environment and a significant contradiction between human and land (Shen et al., 2023). Designated as an apple eugenic zone by the United Nations, the plateau's apple orchards reached 1.33 million  $\text{hm}^2$  (Gao et al., 2021d). In pursuit of improving the yield and economic benefits, the application of fertilizer in apple orchards has steadily increased over year, peaking at  $543 \text{ kg N ha}^{-1}$  in 2017 (Zhu et al., 2021). According to the statistics of the land use type map (Fig. 1), apple orchards and cropland accounted for 51.1 % and 46.0 % of the agricultural area, respectively. The population density here is about  $300 \text{ people km}^{-2}$ , which is a high-density population area on Loess Plateau. The catchment is a typical headwater catchment bounded by watersheds and an outlet section. Its downstream mainstream, Heihe River, is designated as a national first-class drinking water source protection zone, requiring higher water quality standards. The local monitoring showed that the water table is about 80 m deep. The maximum height difference from the tableland to the bottom of gully is 280 m, while the tableland is at an altitude of 1220 m. The wet season is from May to October, while the dry season is from November to April. Additional information on the climate, topography, land use and soil texture of Wangdonggou catchment can be found in Section 1 of Supporting Information.

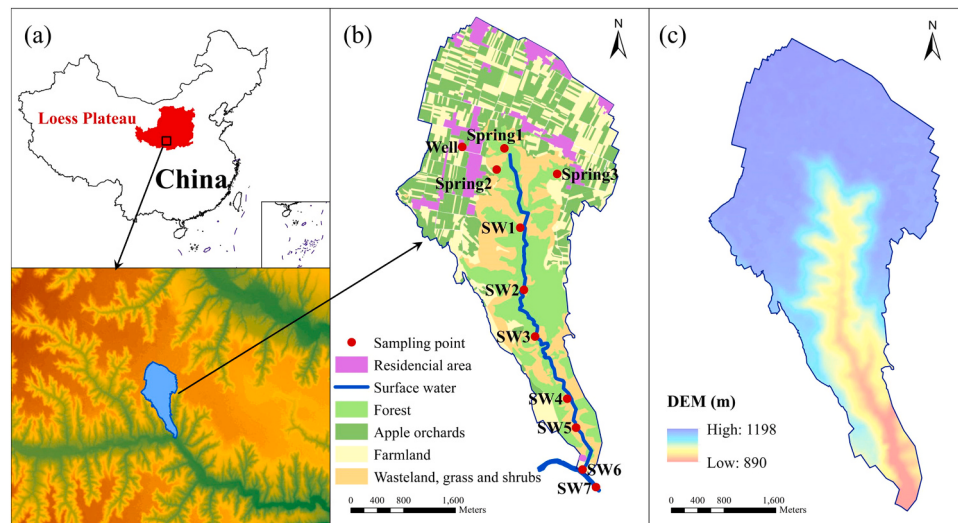


**Fig. 1.** (a) The location, (b) land use and sampling sites, and (c) digital elevation model (DEM) of Wangdonggou catchment ( $8.3 \text{ km}^2$ ). SW represented surface water.

## 2.2. Questionnaire survey and sample collection

A field questionnaire survey was implemented in Wangdonggou catchment from June to December 2020 to investigate the N balance in apple orchards. A household interview was adopted to ensure the effectiveness and accuracy of the investigation. The sample size of the questionnaire was 130, among which 104 were valid questionnaires. The investigation contents included the planting area of apple orchards, apple tree varieties, tree age, planting density, yield, fertilization time and method, types and amounts of chemical and organic fertilizers, etc. Basic data of croplands for N balance was derived from the relevant articles completed in this catchment (Liu et al., 2014; Liang et al., 2016; Nan et al., 2016; Yao et al., 2017; Wang et al., 2020; Zhang et al., 2021a; Fu et al., 2022). The equation for agricultural N balance can be found in Section 2 of Supporting Information. Soil samples at 0–10 m depth from multi-year's croplands and 12-, 20-, and 24-year-old apple orchards were collected to determine soil  $\text{NO}_3^-$  contents. Other details of survey information as well as the soil sample collection and testing can be found in other papers of ours (Ren et al., 2023).

Water samples from surface water, groundwater, and precipitation in the catchment from April 2021 to November 2022 were collected in this study. To facilitate sampling and ensure route safety, surface water sampling points were set up at intervals of 500–1000 m. The seven surface water sampling sites from top to bottom include upstream (SW1), middle and upper reaches (SW2), middle and lower reaches (SW3), control stations (SW4), downstream (SW5), the outlet (SW6) and the Black River (SW7) (the river after confluence). The four groundwater sampling sites include three springs (Spring 1, Spring 2, and Spring 3) located at different locations at the junction of the agricultural area and the gully area, and one deep well located in the agricultural area (Fig. 1). Well water and spring water represent distinct discharge forms of groundwater. Well water is obtained through artificial excavation, while spring water emerges via natural discharge at the land surface under the influence of gravity or hydrogeological pressure. A precipitation collection point was set up near the well. Surface water and groundwater samples were collected monthly to investigate seasonal variations. During rainfall events, precipitation, and water samples from SW6 and SW7 were collected to examine surface water recharge dynamics and nitrogen transport patterns under different hydrological recharge conditions. All water samples were immediately sealed and stored at  $4^\circ\text{C}$ . Water quality indexes determined in this study include  $\text{NO}_3^-$ ,  $\text{NH}_4^+$ , TN, Cl<sup>-</sup>,  $\delta^{15}\text{N-NO}_3^-$ ,  $\delta^{18}\text{O-NO}_3^-$ ,  $\delta^{2}\text{H-H}_2\text{O}$  and  $\delta^{18}\text{O-H}_2\text{O}$ . Details of water sample collection and treatment, determination analysis of hydrochemical indexes and stable isotopes can be found in Section 3 of

## Supporting Information.

## 2.3. Bayesian stable isotope mixing model (MixSIAR)

To estimate the contribution of nitrate sources in the water, the latest Bayesian mixing model (MixSIAR) in R was used in this study for stable isotope analysis. MixSIAR is a new generation stable isotope mixing model based on R, integrating the advantages of many other Bayesian mixing models (MixSIR, SIAR and SIMMR). Indeed, the key advantage of MixSIAR is the ability to include fixed and random effects as covariates explaining variability in mixture proportions, and to enhance the model robustness by stabilizing parameter estimation with prior and posterior distributions (Stock et al., 2018). The key parameters of the MixSIAR model include three components: source data, discrimination data and mix data. The source data comprises the isotopic means (Mean) and standard deviations (SD) of each source. The discrimination data refers to the isotopic discrimination factors, typically derived from literature or experimental data. The mix data consists of the isotope values of the target sample (Chen et al., 2024a). MixSIAR computes the proportional contributions of potential sources to the mixtures (samples) through their tracers (generally stable isotopes) based on the mass conservation equation shown below (He et al., 2022):

$$X_{ij} = \sum_{k=1}^{n_s} p_{ik} S_{kj} + \varepsilon_{ij} \quad (2)$$

where  $X_{ij}$  represents the value of the  $j^{\text{th}}$  tracer (isotopic composition) for the  $i^{\text{th}}$  sample;  $n_s$  represents the number of sources;  $p_{ik}$  represents the proportional contribution of the  $k^{\text{th}}$  source to the  $i^{\text{th}}$  sample;  $S_{kj}$  represents the value of the  $j^{\text{th}}$  tracer in the  $k^{\text{th}}$  source;  $\varepsilon_{ij}$  represents the error of the  $j^{\text{th}}$  tracer (isotopic composition) for the  $i^{\text{th}}$  sample. More details of this model can be found in Torres-Martinez et al. (2020) and Stock et al. (2018). In this study, the  $\delta^{15}\text{N}$  and  $\delta^{18}\text{O}$  ranges of  $\text{NO}_3^-$  derived from DN were measured by 66 precipitation samples. The  $\delta^{15}\text{N}$  and  $\delta^{18}\text{O}$  ranges of  $\text{NO}_3^-$  derived from FN, SN and MN refer to Gao et al. (2021c) whose study area has the similar soil texture, fertilization structure and rural population as this study area (Table. S1).

## 2.4. Uncertainty

Uncertainty is a key problem to be considered in the quantitative identification of nitrate sources. The sum of the ratios of all nitrate sources is 1. However, as a random statistical variable, the estimated contribution ratio of each source should be a probability distribution within a certain range. The Markov chain Monte Carlo mixed model of

the MixSIAR model can provide the probability density function of the proportion of contributions from different sources (Fig. S2). Therefore, this study referred to the uncertainty index (UI) proposed by Ji et al. (2017) to characterize the uncertainty degree of the dual isotope method to the output results of the MixSIAR. UI means the difference between the proportional contribution of the maximum and minimum value of the rapid growth segment of the 90 % cumulative probability in the cumulative distribution function divided by 90, that is, the difference between the contribution proportion of the 95 % and 5 % quantile divided by 0.9 (Shang et al., 2020; Torres-Martínez et al., 2021). A smaller UI value indicates a more stable contribution from the source, while a larger value indicates greater variability of the contribution from the source.

Data were statistically analyzed using SPSS 21.0 (IBM Corp., Armonk, NY, USA). ArcGIS 10.2 was used to construct the maps in Fig. 1. Origin Pro 8.0 (Origin Lab Corporation, MA, USA) was used to prepare the other figures.

### 3. Results

#### 3.1. Agricultural N balance and soil nitrate accumulation

The total input of N in apple orchards was fourfold the amount that required for apple tree growth, with 87.1 % from fertilizer. This excessive input led to significant surplus of N, accounting for 75 % of the total N input, resulting in approximately  $847.4 \text{ kg} \cdot \text{ha}^{-1}$ .N being released into surrounding environment annually. Of this, 51.1 % ( $609.5 \text{ kg} \cdot \text{ha}^{-1}$ ) accumulated as  $\text{NO}_3^-$  in soil, while 19.9 % ( $237.88 \text{ kg} \cdot \text{ha}^{-1}$ ) was lost through runoff (Fig. 2a). In cropland, N input to was predominantly from fertilizer, supplemented by 15.7 % from atmospheric nitrogen deposition. The N needed for crop output and strew-N accounted for 71.5 % of the total N input, leaving a N surplus of only 28.5 %. The crop output in apple orchards was 1.75 times higher than in cropland, whereas the total N input was 4.01 times that of croplands, with soil N residue being 35.2 times higher. The runoff loss of N in apple orchards were 3.7 times higher compared to croplands.

The soil  $\text{NO}_3^-$  accumulation in cropland was predominantly concentrated within 0–1 m depth, whereas in apple orchards, it extended to the 0–6 m depth and reached its peak at 1–2 m depth (Fig. 2b). The soil  $\text{NO}_3^-$  accumulation at 0–6 m depth in 24-year apple orchards was  $1336.8 \text{ kg N} \cdot \text{ha}^{-1}$ , 28 times greater than that in croplands.

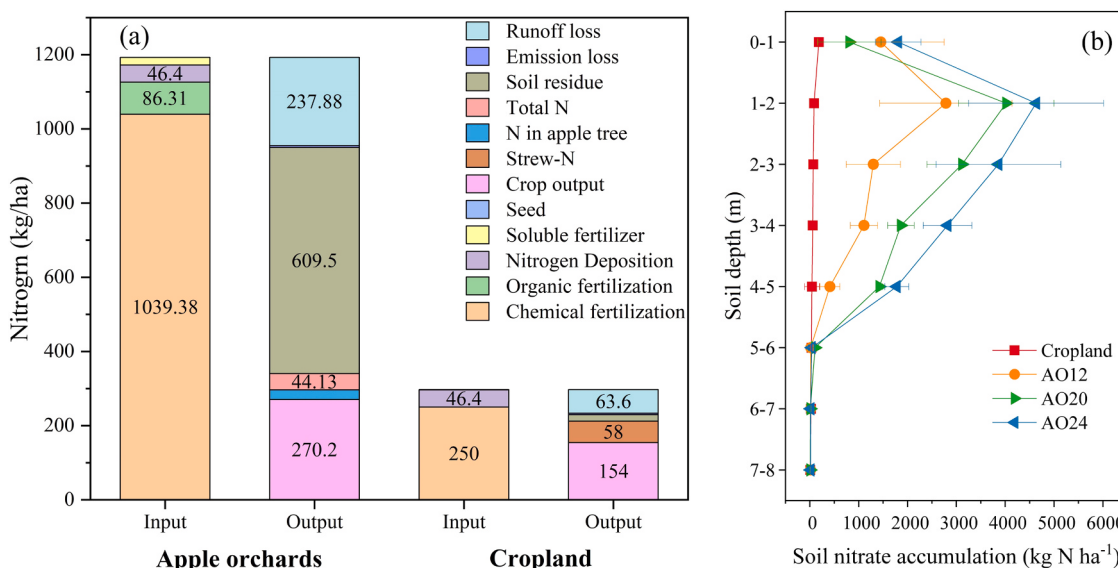


**Fig. 2.** Nitrogen balance (Input, Output and Surplus) (a) and soil nitrate accumulation (b) of apple orchards and cropland in Wangdonggou catchment. AO represent apple orchards and the number after AO represents the age of the apple orchards.

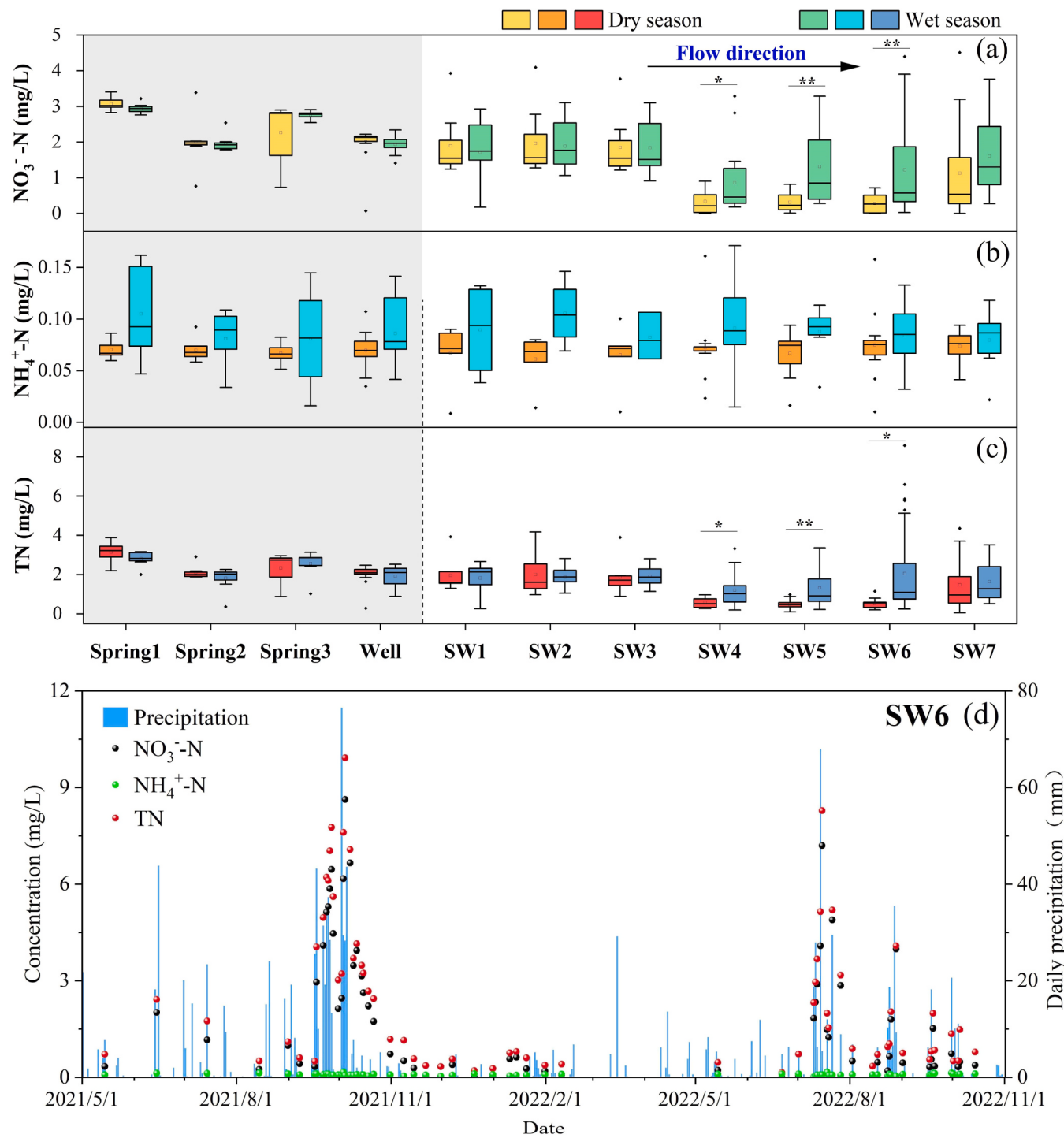


**Fig. 3.**  $\text{NO}_3^-$ -N (a),  $\text{NH}_4^+$ -N (b), TN (c) concentration in surface water and groundwater in dry and wet season; daily precipitation and N concentration of different forms in SW6, the surface water outlet in Wangdonggou catchment (d), from 2021 to 2022. SW represented surface water. The difference between dry season and wet season was determined by independent sample t test, with \*, \*\* and \*\*\* representing  $p < 0.05$ ,  $p < 0.01$  and  $p < 0.001$ , respectively.

region than in dry season (Fig. 4e). Similarly, the number of SW6 points entering the FN region was greater during rainfall than during non-rainfall in wet season, and higher than during non-rainfall in dry season (Fig. 4f). Furthermore, almost no points were distributed in denitrification region in Fig. 4d, e, f. The correlation coefficient between  $\ln \text{NO}_3^-$  and  $\delta^{15}\text{N-NO}_3$  in groundwater was 0.077, and 0.245 between  $\ln \text{NO}_3^-$  and  $\delta^{18}\text{O-NO}_3$ . Meanwhile, in surface water, these values were 0.097 and 0.021, respectively (Fig. 5). The  $R^2$  of fitting curves between  $\ln \text{NO}_3^-$  and  $\ln \text{NO}_3^-$  and between  $\delta^{15}\text{N-NO}_3$  and  $\delta^{18}\text{O-NO}_3$  of surface water

were less than 0.1 in both dry and rainy seasons and during both rainfall and non-rainfall periods. Similarly, the  $R^2$  of groundwater was also less than 0.1 (Fig. S3-S5).

The nitrate source and contribution ratio of different sources in groundwater remained stable throughout the whole year, with the proportion of MN consistently exceeding 98 % (Fig. 6). In SW1, SW2, SW4 and SW6, the contribution ratio of different nitrate sources showed minimal variation between the dry and wet season, with MN consistently accounting for over 90 %, significantly higher than fraction of FN,

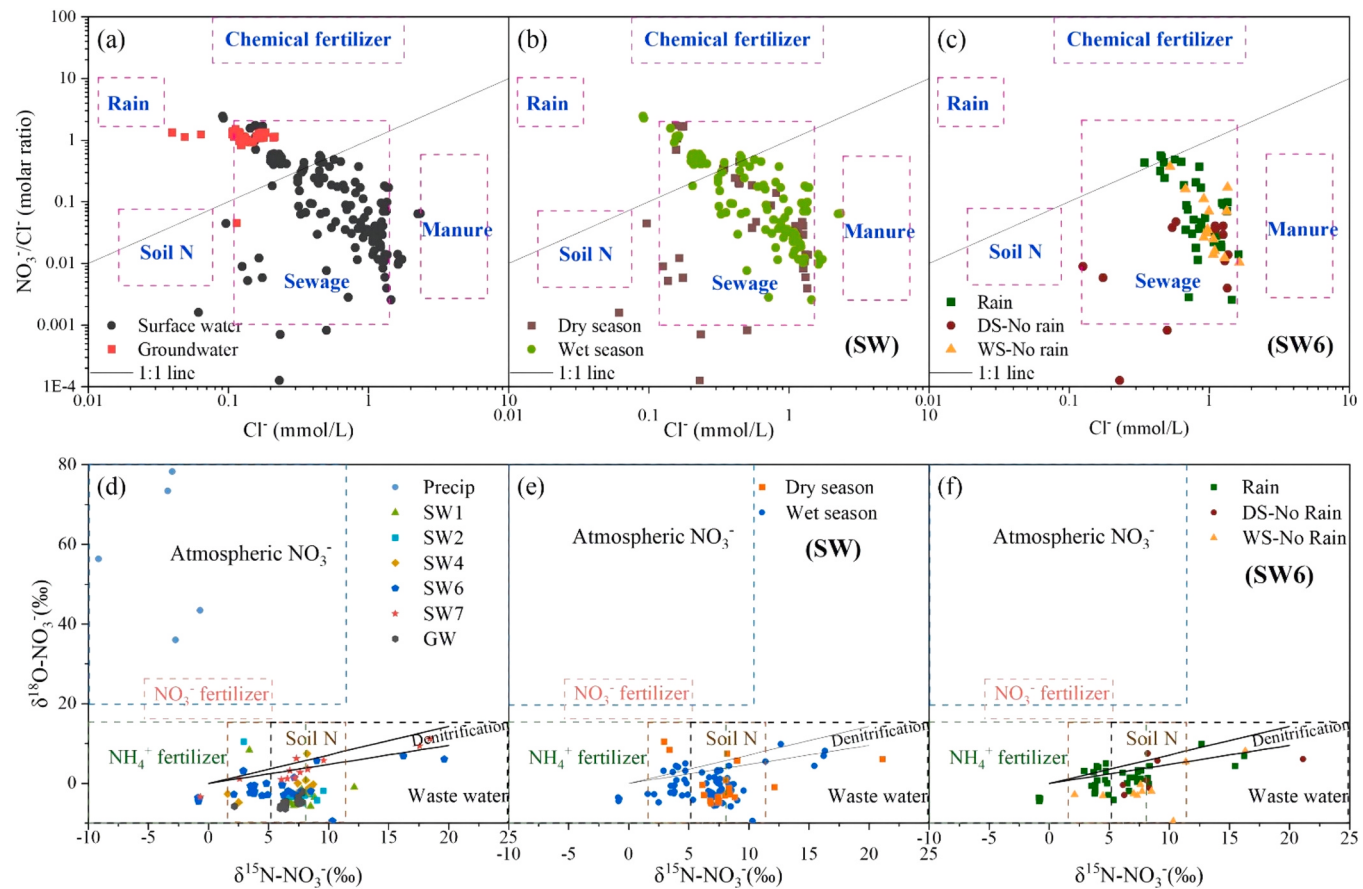


**Fig. 4.** Relationships between  $\text{NO}_3^-/\text{Cl}^-$  and  $\text{Cl}^-$  concentration (a,b,c), and dual  $\delta^{15}\text{N-NO}_3$ ,  $\delta^{18}\text{O-NO}_3$  (d, e, f) of groundwater (GW), surface water (SW) and precipitation (precip), dry season (DS) and wet season (WS) of surface water, and during rainfall and non-rainfall at surface water outlet (SW6). Data in (a) were adapted from Zhu et al. (2023) and Torres-Martínez et al. (2021). The range of  $\delta^{15}\text{N-NO}_3$  and  $\delta^{18}\text{O-NO}_3$  values for different nitrates was organized according to Xue et al. (2009) and Hu et al. (2019).

SN and DN. However, the proportion of MN gradually decreased, while the combined proportion of SN, FN and DN gradually increased along the water flow direction (SW1: < 5%; SW7: 6.4%–18.5%).

In contrast to the non-rainfall period of SW6, where over 90% of  $\text{NO}_3^-$  originated from MN, the source of  $\text{NO}_3^-$  underwent significantly changes during rainfall events (Fig. 6). Intriguingly, as daily precipitation increased, the proportion of  $\text{NO}_3^-$  from MN notably decreased, while the combined proportions from FN and SN exhibited a significantly increase. Conversely, as daily precipitation decreased, the proportion of  $\text{NO}_3^-$  from MN experienced a sharp rebound, while the combined proportions from FN and SN gradually decreased. In few samples with low precipitation that day, the combined ratio of FN and SN remained high due to the short time elapsed since the cessation of the heavy precipitation.

The uncertainty analysis (Table 1) showed that among the four nitrate sources, DN had the lowest UI with an average value of 0.022, while MN had the highest UI with an average value of 0.243. The UI of FN and SN were between DN and MN. The UI of groundwater was significantly lower than that of surface water. SW6 and SW7 were higher than other surface water points, while the UI of SW6 in rainfall period was higher than that in non-rainfall period.

#### 3.4. Water source identification and water cycle characteristics

The slope of surface water (6.37) fell between LWML (7.40) and groundwater (3.12) (Fig. 7a). During the wet season, the surface water slope (6.63) was positioned between LWML (7.40) and dry season surface water (3.74) (Fig. 7b). Furthermore, the slope of SW6 during

rainfall (7.13) exceeding that during non-rainfall in both the wet (5.93) and dry season (4.10) (Fig. 7c). It is noteworthy that surface water in this catchment primarily originated from groundwater, contributing over 80% (Fig. 8). The contribution during wet season was marginally higher than that during dry season.

The contribution of groundwater in SW6 during non-rainfall was also found to be over 80% (Fig. 8). As daily precipitation increased, the contribution of groundwater decreased while the contribution of precipitation increased significantly. Conversely, with a decrease in daily precipitation, the contribution of groundwater rebounded sharply, and the contribution of precipitation dropped to the non-rainfall level. In few samples with low precipitation that day, the proportion from rain remained high due to the short time since the end of the heavy precipitation. The highest contribution of precipitation to surface water reached 66.2% during rainfall periods.

## 4. Discussion

### 4.1. Fate of agricultural surplus N

N balance is one of the reliable methods to evaluate the input, output and surplus of N in agricultural production systems (Gao et al., 2021c). The results of N balance in this study showed that the excessive application of N fertilizer in apple orchards resulted in N input 4 times that required for apple growth, while the N input in croplands was only 1.4 times that for crop out (Fig. 2a). Among the multiple destinations of surplus N in apple orchards, nitrate as the main form of N stored in deep soil accounted for the highest proportion (51.1% in this study) (Fig. 2b),

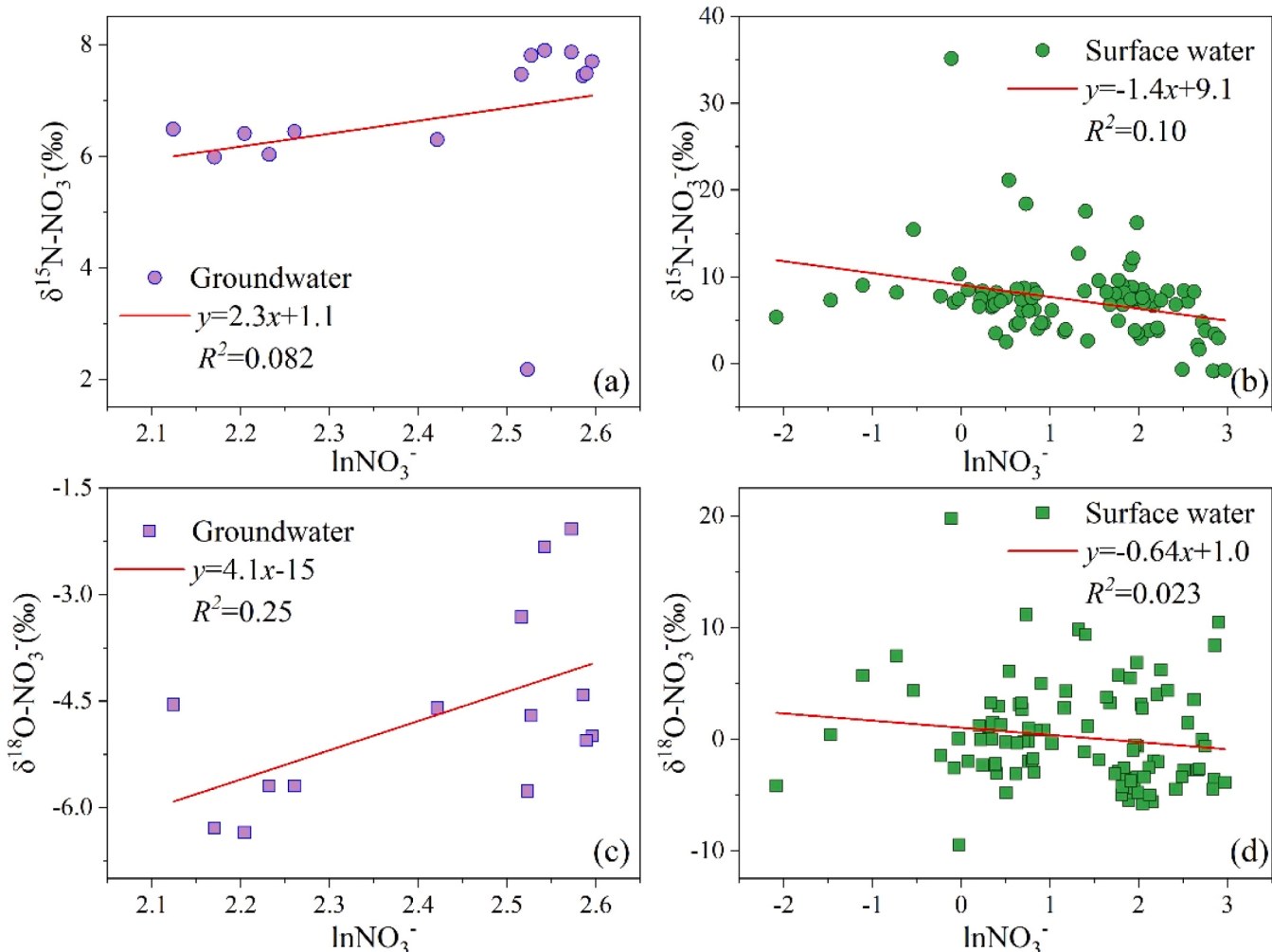


**Fig. 5.** Relationship between  $\ln\text{NO}_3^-$  (the logarithm base 10 of the  $\text{NO}_3^-$  concentration) and  $\delta^{15}\text{N-NO}_3^-$  (‰) and  $\delta^{18}\text{O-NO}_3^-$  (‰) in groundwater and surface water. (a) and (c) are groundwater points, and (b) and (d) are surface water points.

which has been widely concerned and studied (Huang et al., 2021; Zhu et al., 2022). However, N loss through runoff was often ignored. The potential N loss through runoff in apple orchard of the study area was as high as  $199.75 \text{ kg-ha}^{-1}\text{-year}^{-1}$ , which accounted for 19.9 % of N input and 3.7 times that of cropland (Fig. 2a). Miao et al. (2023) also found that N loss in apple orchards in this region through ways other than soil accumulation and gas emission accounted for 22.9 % of N input, reaching  $113.92 \text{ kg-ha}^{-1}\text{-yr}^{-1}$ . These potential N losses through runoff may enter groundwater and surface water through different hydrological paths, resulting in an increase in their N concentration (Wang et al., 2021; Yan et al., 2023).

In intensive agricultural areas with high fertilization rate, the high residual and the lag effect of soil N are the main factors contributing to the failure of surface water N management to achieve desired water quality goals (Zhou et al., 2023). In areas where  $\text{NO}_3\text{-N}$  is the main form of soil inorganic N, soil  $\text{NO}_3^-$  accumulation was often accompanied by significant excess of  $\text{NO}_3^-$  in groundwater or surface water (Ezzati et al., 2023). However, in this study, the  $\text{NO}_3\text{-N}$  concentrations in both groundwater and surface water remained below the World Health Organization (WHO) drinking water threshold ( $10 \text{ mg-L}^{-1}$ ) for most of the year, despite apple orchards with severe N surpluses occupying 54 % of the agricultural area of the catchment and the soil nitrate accumulation of 24-year apple orchards at 0–6 m depth reaching  $1336.8 \text{ kg N-ha}^{-1}$  (Figs. 1, 2). Notably, during heavy precipitation, there were significant fluctuations in  $\text{NO}_3\text{-N}$  concentrations of surface water, with the highest

recorded concentration reaching  $8.63 \text{ mg-L}^{-1}$ . This N concentration level was close to the drinking water safety threshold of WHO and posed a potential pollution threat to the downstream mainstream Heihe River, which has been designated as a national first-class drinking water source protection zone (Fig. 3). Under climate conditions with increasingly frequent extreme precipitation events, the  $\text{NO}_3^-$  concentration of surface water is highly likely to exceed the established safety threshold (Park et al., 2016). Consequently, identifying the primary sources and key transport pathways of nitrate in the groundwater and surface water, especially during periods of heavy rainfall, is essential for exploring the impact of agricultural excess nitrogen on water nitrogen pollution in this area.

#### 4.2. Nitrate sources of water and the contribution ratio of different sources

The relationship between  $\text{NO}_3^-/\text{Cl}^-$  molar ratio and  $\text{Cl}^-$  concentration and the relationship between  $\delta^{15}\text{N-NO}_3^-$  and  $\delta^{18}\text{O-NO}_3^-$  are widely used for qualitative analysis of nitrate sources in natural water bodies (Torres-Martínez et al., 2021; Ren et al., 2022). In the nitrate source traceable maps of this study, the groundwater points were concentrated in the Sewage area or the overlapping area of SN, FN and MN (Fig. 4a, d), indicating that the concentration and source of  $\text{NO}_3^-$  in groundwater were very stable, and domestic sewage was the main nitrate source. The quantitative analysis of MixSIAR showed that there was almost no  $\text{NO}_3^-$

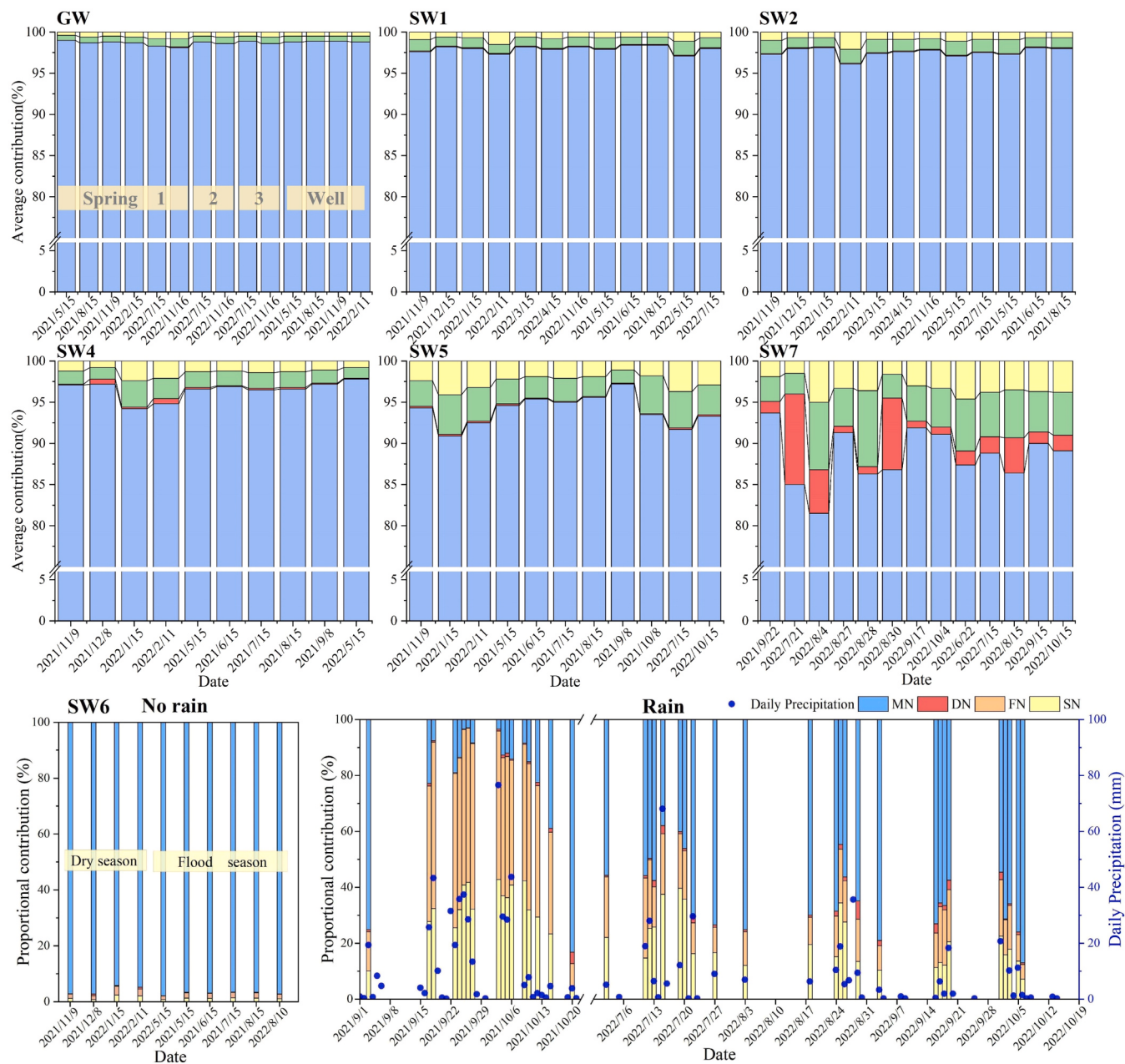


**Fig. 6.** Nitrate source contributions in Wangdonggou catchment: seasonal variations for groundwater (GW) and surface water (SW1,2,4,5,7), and rainfall-driven fluctuations (No rain/Rain) at the catchment outlet (SW6). MN represented manure and sewage; DN represented atmospheric deposition; FN represented chemical fertilizer; SN represented soil nitrogen.

**Table 1**

Uncertainty index of each  $\text{NO}_3^-$  source at different sampling sites.

Nitrate source	UI						
	SW1	SW2	SW4	SW6	SW7	GW	Average
Atmospheric deposition (DN)	0.015	0.018	0.016	0.032	0.049	0.085	0.036
Chemical fertilizer (FN)	0.067	0.072	0.137	0.231	0.211	0.100	0.136
Manure and sewage (MN)	0.112	0.121	0.225	0.590	0.335	0.046	0.238
Soil nitrogen (SN)	0.053	0.059	0.075	0.572	0.162	0.032	0.159

from FN in groundwater throughout the year (Fig. 6). This finding indicated that  $\text{NO}_3^-$  from residual fertilizer in apple orchards and croplands had not yet reached into groundwater. This was different from that in agricultural areas with shallow groundwater level, soil residual  $\text{NO}_3^-$

there can easily enter groundwater and caused the concentration to exceed the safety threshold (Cameira et al., 2021; Gao et al., 2024). In areas with abundant precipitation and irrigation conditions, heavy precipitation and irrigation would accelerate  $\text{NO}_3^-$  into groundwater,

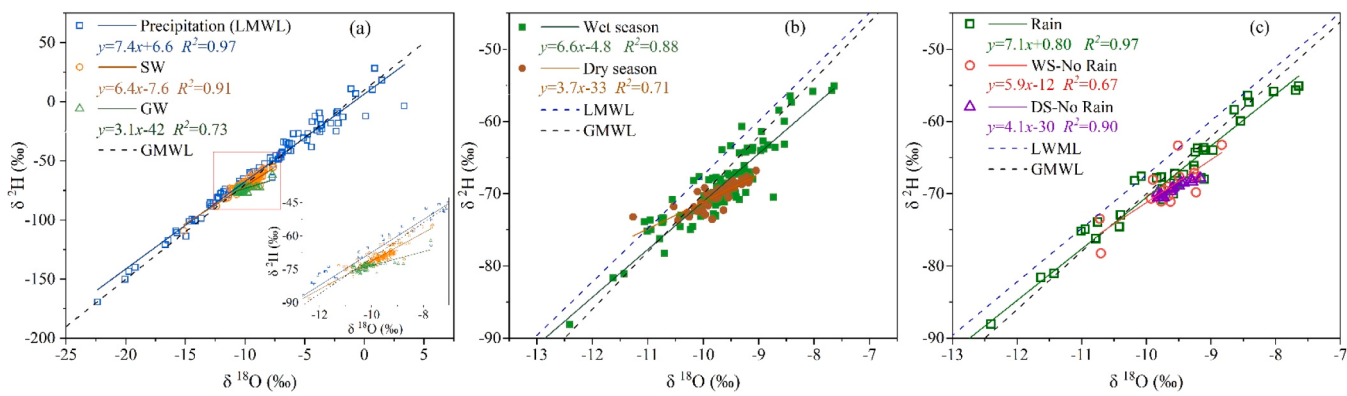


**Fig. 7.** Dual  $\delta^2\text{H}-\text{H}_2\text{O}$  and  $\delta^{18}\text{O}-\text{H}_2\text{O}$  of groundwater (GW), surface water (SW) and precipitation (LWML, local meteoric water line) (a), dry season (DS) and wet season (FS) of surface water (b), and during rainfall and non-rainfall at surface water outlet SW6 (c). Relationships between  $\delta^{18}\text{O}-\text{H}_2\text{O}$  and d-excess of groundwater, surface water and precipitation (d). (GMWL, global meteoric water line, sourced from: Craig, (1961)).

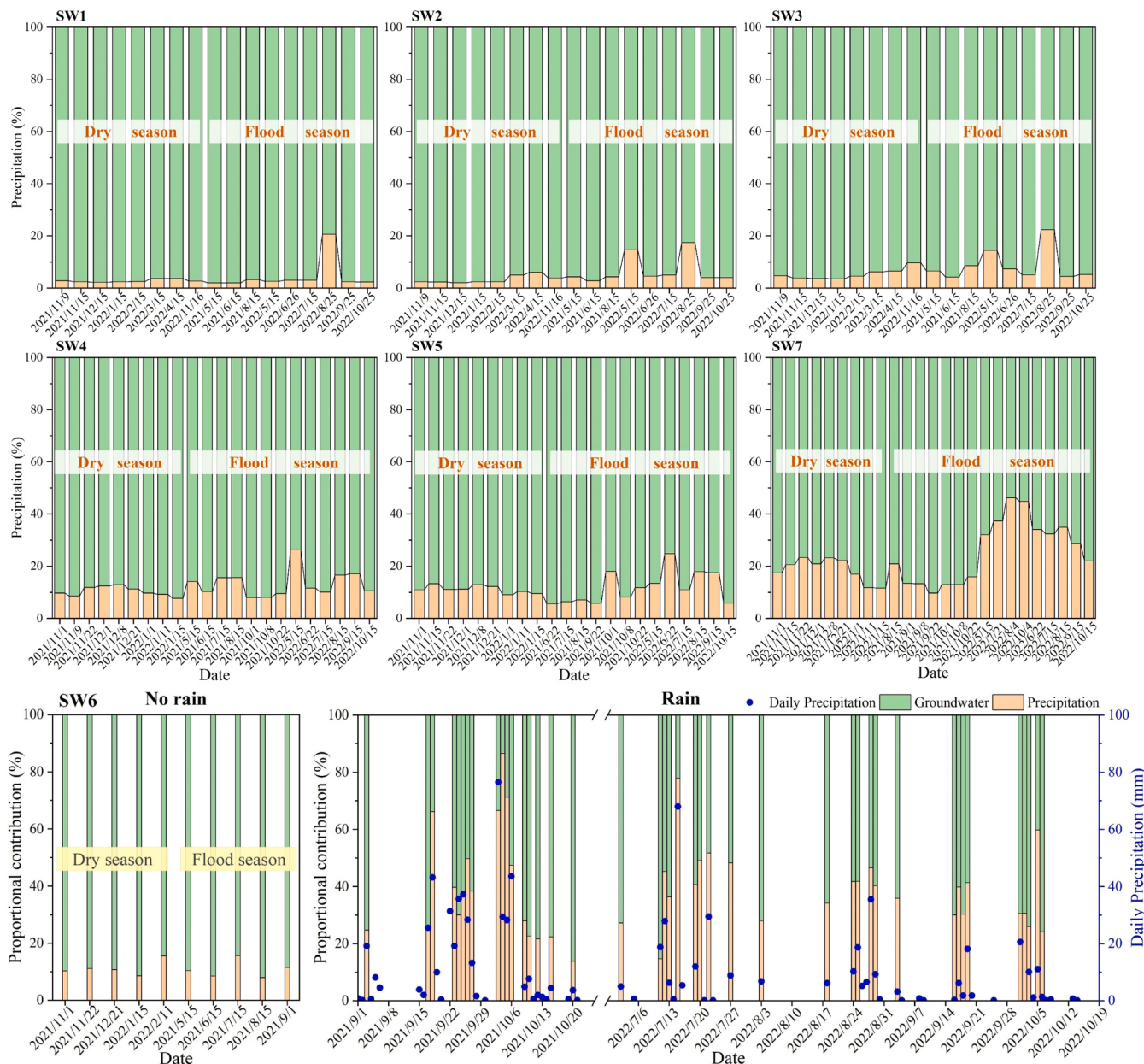


**Fig. 8.** Contribution of precipitation and groundwater to surface water in SW6 during rainfall and non-rainfall periods 2020–2021.

even in areas with vadose zone thickness up to 5–100 m (Gao et al., 2021c; Sun et al., 2024). In addition, the results revealed that around 98 % of  $\text{NO}_3^-$  in groundwater was derived from MN (Fig. 6). This was similar to the findings of Niu et al. (2022) in groundwater in the southern part of the study area, who believed that these  $\text{NO}_3^-$  came from pre-modern agricultural activities and historical  $\text{NO}_3^-$  loads generated by domestic waste.

The points distribution of surface water was scattered, and most of them was also distributed in the Sewage area (Fig. 4b), indicating that domestic sewage is also an important source of  $\text{NO}_3^-$  in surface water. In Fig. 4d, e, f, the number of surface water points entering the FN region was higher in wet season than in dry season, and the rainfall period in the wet season was higher than the non-rainfall period in the wet season and higher than the non-rainfall period in the dry season. This indicated that the contribution of fertilizer to nitrate source reached the highest when the precipitation occurred in wet season. The quantitative analysis of this study found that  $\text{NO}_3^-$  concentration of surface water and the proportion of different nitrate sources had a strong response to heavy precipitation. In particular, the total  $\text{NO}_3^-$  ratio from FN and SN increased rapidly with the increase of daily precipitation, and gradually recovered with the end of heavy precipitation events (Fig. 6), which was similar to the change pattern of surface water runoff (Jiao et al., 2015). Studies have also shown that monthly river TN emissions in agricultural watershed was influenced by a combination of hydrology, including heavy rainfall events, and anthropogenic controls, including fertilization (Xie et al., 2022; Xiao et al., 2019). However, similar to groundwater, in most of the time without precipitation, the proportion of MN in surface water was stable at more than 90 %, indicating that MN was also an important source of  $\text{NO}_3^-$  in surface water (Fig. 6). Consequently, it can be inferred that the source of  $\text{NO}_3^-$  in surface water of the catchment was strongly affected by heavy precipitation, and the hydrological connectivity between groundwater and surface water lead to the interrelation of  $\text{NO}_3^-$  dynamic changes between them (Tillman et al., 2016). In order to understand the driving mechanism of NPS pollution of N, it was necessary to further analyze the water cycle pattern and the conversion relationship between different water bodies of this catchment (Wang et al., 2024).

Strong denitrification processes can significantly influence  $\delta^{15}\text{N}$ - $\text{NO}_3^-$  and  $\delta^{18}\text{O}-\text{NO}_3^-$ , resulting in an increase in  $\delta^{15}\text{N}$  and  $\delta^{18}\text{O}$  values and an exponential decrease in  $\text{NO}_3^-$  concentration. These changes are crucial indicators for evaluating denitrification process in soil and water systems (Xue et al., 2009). However, there was no correlation between  $\ln \text{NO}_3^-$  and  $\delta^{15}\text{N}-\text{NO}_3^-$  as well as  $\delta^{18}\text{O}-\text{NO}_3^-$  was observed both in the groundwater and surface water, regardless of the wet or dry seasons or the presence of precipitation (Fig. 5, S1-S3). This indicated that denitrification has little effect on the isotopic composition of  $\text{NO}_3^-$  in both groundwater and surface water. Yu et al. (2020) also observed that the denitrification of groundwater and surface water in this region was weak. However, even in oxygen-rich rivers, the sediment may be sub-oxidized or anoxic, and there may also be opportunities for denitrification. But it had little effect on the isotopic fractionation of  $\text{NO}_3^-$  in the entire oxygen-rich rive (Wei et al., 2022).

#### 4.3. The driving mechanism of agricultural N pollution of NPS

Stable water isotopes are effective tracers for the identification of river water sources, hydrological pathways, hydrological connectivity, and the spatiotemporal variations of hydrological processes, especially for rivers that lack continuous runoff monitoring data (Hu et al., 2020; Hamidi et al., 2023b). In this study, the  $^2\text{H}-\text{H}_2\text{O}$  and  $^{18}\text{O}-\text{H}_2\text{O}$  isotopes of groundwater, surface water and precipitation and MixSIAR models were used to elucidate the water cycle characteristics of the catchment and hydrological connectivity between groundwater and surface water. Surface water was recharged by precipitation and groundwater, as evidenced by the fitted line slope falling between those of precipitation and groundwater (Fig. 7) (Hamidi et al., 2023a). Based on the view of Warix

et al. (2023) that surface runoff and rapid subsurface lateral flow in upper soil represent young water, and groundwater represents old water, this study found that surface water received a higher proportion of new water following heavy rainfall compared to non-rainfall periods, as well as during wet season compared to dry season (Fig. 8). This was consistent with the general hydrological recharge law of surface water under different seasons and precipitation conditions (Chittolina et al., 2023). Moreover, during non-rainfall periods, over 80 % of the surface water was composed of old water. During periods of rainfall, the contribution of new water in surface water exhibited a sharp increase with precipitation intensity, reaching up to 66.2 %, and returned to non-rainfall level once runoff generation ended (Fig. 8). However, in areas with abundant precipitation or strong soil permeability where the old water was also the main contributor to surface water, heavy precipitation easily passed through the soil into groundwater. Its groundwater level was easily affected by heavy precipitation and the average age of groundwater was relatively young (Xiao et al., 2022; Chittolina et al., 2023). In irrigated agricultural catchments, irrigation water may also become one of the sources of surface water, and its contribution rate to surface water could even exceed that of groundwater and surface runoff in the period of high irrigation volume (Lv et al., 2018). The clarity of the hydrological process in the catchment helps to further explore the transport path of  $\text{NO}_3^-$ .

Therefore, the mechanism of N pollution of NPS in rain-fed agricultural catchment with deep vadose zones has been elucidated. For groundwater,  $\text{NO}_3^-$  from soil residual fertilizer in apple orchards and cropland has not entered groundwater. This was due to the deep vadose zone causing an overly long vertical transport path (Turkeltaub et al., 2021) and the lack of sufficient downward driving force for  $\text{NO}_3^-$  from soil residual fertilizer (Wells et al., 2021). Huang et al. (2020) found that the infiltration rate of soil water in Loess Plateau with a depth of 40–75 m in the unsaturated zone was only  $0.12\text{--}0.14 \text{ m yr}^{-1}$ , and the ages of groundwater ranged from hundreds of years to 20,000 years. As a result, there has been no rapid modern recharge of groundwater since the 1950s. In Los Alamos Canyon of the United States, where the climate was semi-arid and vadose zone thickness was 100–375 m, the mesa-top infiltration rate was only about  $1 \text{ mm yr}^{-1}$ , while the impact of occasional transient infiltration events caused by climate or human activities could last for ten years or longer (Broxton and Vaniman, 2005; Robinson et al., 2005). Therefore, the current  $\text{NO}_3^-$  of groundwater in the catchment primarily originated from the residual domestic sewage and manure from historical agricultural periods retained in the soil close to the aquifer (Niu et al., 2022), and such pollution would be persistent. And even during heavy precipitation occurred in the rainy season, soil water did not enter groundwater through deep infiltration, nor did FN enter groundwater. Therefore, the results of groundwater were inconsistent with the hypothesis that deep soil and limited precipitation did reduce the speed and intensity of N release into groundwater, leaving little N from excess fertilizers to enter the groundwater so far.

However, for surface water, during heavy precipitation in the wet season, plenty of infiltration excess runoff generated on both tableland and slope, carrying a large amount of  $\text{NO}_3^-$  from residual fertilizer and soil into the surface water (Li et al., 2009). Consequently, the proportion of  $\text{NO}_3^-$  from FN and SN rose with the increase of surface runoff. This disrupted the stable pattern where MN typically constituted the majority of the nitrate source in non-rainfall periods (Fig. 6). Due to the typical lag between the end of heavy precipitation and the end of runoff production (Asano and Uchida, 2018), the nitrate source of surface water was not immediately dominated by MN at the conclusion of heavy precipitation. Instead, the proportion sum of FN and SN gradually declined, and the nitrate source gradually recovered to be dominated by MN (Fig. 6). Since surface water was mainly replenished by groundwater (Figs. 7,8) during periods unaffected by heavy precipitations, MN was also the main nitrate contributor of surface water (Fig. 6). Therefore, the results of surface water confirmed the hypothesis, that is, although deep soil and limited precipitation reduced the speed and intensity of N

release to water, agricultural surplus N still entered surface water during heavy precipitation, making fertilizer an important part of nitrate source in surface water.

Additionally, the higher recharge proportion of new water in the mainstream (SW7) compared to SW1-SW6 (Fig. 8) was because the mainstream gathered surface water from all upstream catchments. As a result, it was more responsive to new water and more susceptible to pollutants released from numerous agricultural catchments upstream after heavy precipitation (Baldwin et al., 2016). Consequently, the annual mean and maximum  $\text{NO}_3^-$  concentration in SW7, as well as the proportion of  $\text{NO}_3^-$  from DN, FN and SN, were significantly higher than those in SW1-SW6 (Fig. 6).

#### 4.4. Uncertainty and suggestion

Evaluating the uncertainty of simulation results is an important step in model research (Matsuzaki and Kubota, 2024). The uncertainty analysis results for quantitative  $\text{NO}_3^-$  traceability showed that the UI value of DN was the smallest, MN was the largest, FN and SN were between DN and MN (Table 1). The UI values of the four nitrate sources in this study were all lower than those of the drinking water source area in Shanxi, which was in the subtropical humid area (Shang et al., 2020). Since the fractionation of  $\delta^{2\text{H}}\text{-H}_2\text{O}$  and  $\delta^{18\text{O}}\text{-H}_2\text{O}$  mainly occurred in the process of evaporation and condensation (Angert et al., 2004), there is almost no fractionation in the process of storm runoff and groundwater entering surface water. The difference of the  $\delta^{2\text{H}}\text{-H}_2\text{O}$  and  $\delta^{18\text{O}}\text{-H}_2\text{O}$  values of precipitation or groundwater between different sampling points can also be ignored. In addition, denitrification had little effect on  $\delta^{15\text{N}}\text{-NO}_3^-$  and  $\delta^{18\text{O}}\text{-NO}_3^-$  values of surface and groundwater in the study area under different seasons, rainfall, or non-rainfall conditions (Figs. 5, S1–3). Therefore, the uncertainty in the quantitative simulation of nitrate sources was mainly caused by the unavoidable spatio-temporal variations of  $\delta^{15\text{N}}$  and  $\delta^{18\text{O}}$  eigenvalues of the four  $\text{NO}_3^-$  sources (Ji et al., 2017). However, the simulation in this study referred to the  $\delta^{15\text{N}}$  and  $\delta^{18\text{O}}$  eigenvalues in a small basin not far from the study area (Gao et al., 2021b), which inevitably increased the uncertainty of the results. Therefore, in order to further improve the accuracy of quantitative analysis of  $\text{NO}_3^-$  sources, it is recommended that the  $\delta^{15\text{N}}$  and  $\delta^{18\text{O}}$  values of the four nitrate sources under different space-time conditions should be measured in future studies. In addition, one of the main findings of this study was that the nitrate NPS pollution in rain-fed agricultural catchment with deep vadose zone and limited precipitation would be aggravated when heavy precipitation occurred. But the time span of the measured data in this study was only 2 years. Due to the low-frequency nature of extreme precipitation events, the short data duration introduced a degree of uncertainty into the conclusions. Future research could investigate the impact of extreme precipitation on nitrate NPS pollution in the study area over a longer time span at different precipitation recurrence periods.

Therefore, in the agricultural catchments with limited precipitation and thick vadose zone, the heavy precipitation periods were the high-risk periods when the surface water N concentration exceeded the safety threshold. In the context of frequent extreme climate in the future (Park et al., 2016), long-term accumulated agricultural N surplus is easy to cause surface water N pollution positively related to precipitation and precipitation intensity during heavy rainfall, which will seriously threaten the water quality safety of surface water in headwater catchments and downstream. In addition, although the deep vadose zone was a natural buffer zone and the limited precipitation reduced the risk of  $\text{NO}_3^-$  pollution in groundwater, heavy precipitation events were also the key driving force for the soil  $\text{NO}_3^-$  accumulation of this rain-fed agricultural area to gradually enter groundwater through deep leaching or priority flow. In order to prevent and control agricultural NPS pollution in this area, suggestions were as follows. Firstly, since the fundamental measure to prevent and control water  $\text{NO}_3^-$  pollution lies in reducing the agricultural N surplus, guidance on scientific and reasonable

fertilization for farmers should be strengthened, and the reasonable combination of organic and chemical fertilizers should be encouraged (Wang et al., 2022). Secondly, considering the environmental burden, based on the N requirement for apple growth from this study, taking soil residual N and N emissions loss in cropland as the optimal control criteria for N surplus, the recommended nitrogen fertilizer application rate for apple orchards in study area was  $300 \text{ kg N ha}^{-1} \text{ yr}^{-1}$ . According to the N application-yield curves for apple orchards in Loess Plateau (Chen et al., 2024b; Li et al., 2024), the nitrogen application rate at the highest apple yield was between  $240$  and  $360 \text{ kg N ha}^{-1} \text{ yr}^{-1}$ . Thus, the recommended nitrogen fertilizer application rate also fell within the optimal range for yield. Finally, the deep rainwater infiltration and collection technologies suitable for semi-arid hilly areas was suggested in apple orchards and farmlands on slope to intercept the runoff generated by heavy precipitation and reduce the entry of surplus nutrients into surface water (An et al., 2023; Song et al., 2020).

#### 5. Conclusion

This study revealed the hidden nitrate pollution threats in rain-fed agricultural regions with deep vadose zones and limited precipitation by exploring the fate of N surplus and the mechanisms of NPS pollution. Apple orchards were found to be major contributors to the regional N surplus due to excessive fertilization, with annual soil accumulation rates reaching  $551.37 \text{ kg ha}^{-1}$  as  $\text{NO}_3^-$ , significantly higher than traditional croplands. This surplus N lost  $257.88 \text{ kg ha}^{-1}$  N per year through pathways other than soil accumulation, thereby increasing the risk of NPS contamination. Groundwater analyses revealed a stable  $\text{NO}_3^-$  concentration, with 98 %  $\text{NO}_3^-$  originating from domestic sewage, indicating that soil  $\text{NO}_3^-$  still did not enter groundwater. Groundwater analysis revealed that 98 % of  $\text{NO}_3^-$  was from domestic sewage, indicating no groundwater  $\text{NO}_3^-$  contamination from fertilization. Surface water analyses elucidated that over 80 % of surface water during periods without precipitation was from groundwater, with similar  $\text{NO}_3^-$  concentrations. During heavy precipitation, however, the proportion of surface water from precipitation and surface runoff increased significantly with the rise in precipitation. Apple orchards and croplands lost  $\text{NO}_3^-$  from residual fertilizer, while slopes and gullies lost  $\text{NO}_3^-$  from soil. Surface runoff increased the proportion of  $\text{NO}_3^-$  from chemical fertilizer and soil N. Although the deep vadose zone delayed pollution and low precipitation alleviated its intensity, the risk of NPS pollution during heavy precipitation remained significant. Thus, this research highlights the environmental challenges posed by nitrogen surplus in semi-arid agricultural landscapes.

#### CRediT authorship contribution statement

**Mingyi Wen:** Writing – review & editing, Methodology, Conceptualization. **Ruxin Shao:** Writing – review & editing, Data curation. **Changjian Li:** Writing – review & editing, Funding acquisition, Conceptualization. **Xining Zhao:** Writing – review & editing, Funding acquisition, Conceptualization. **Min Ren:** Writing – original draft, Visualization, Software, Methodology, Investigation, Data curation, Conceptualization. **Nanfang Ma:** Software, Data curation. **Liuyang Yu:** Writing – review & editing, Funding acquisition. **Jingdan Zhao:** Investigation. **Ting Yang:** Investigation. **Xiaodong Gao:** Writing – review & editing, Funding acquisition.

#### Declaration of Competing Interest

The authors declare no known competing financial interests or personal relationships that could have appeared to influence the work reported in this paper.

## Acknowledgments

We appreciate the editor and reviewers' professional comments that greatly improved this manuscript. This work was supported by the National Natural Science Foundation of China (42125705, 52209069), National Key Research and Development Program of China (2021YFD1900700), Key Research and Development Program of Shaanxi Province (2021NY-064, 2020ZDLNY07-04), China Postdoctoral Science Foundation (2023M742854), Shaanxi Postdoctoral Research Projects (2023BSHYDZZ90), the Natural Science Basic Research Program of Shaanxi (2023JC-XJ-24) and Shaanxi Key Research and Development Program (2023-ZDLNY-49; 2024NC-ZDCYL-02-04).

## Appendix A. Supporting information

Supplementary data associated with this article can be found in the online version at [doi:10.1016/j.agee.2025.109819](https://doi.org/10.1016/j.agee.2025.109819).

## Data availability

Data will be made available on request.

## References

- An, J., Wang, L.Z., Wu, Y.Z., Song, H.L., Du, X.Y., 2023. Response of nutrient loss to natural erosive rainfall events under typical tillage practices of contour ridge system in the rocky mountain areas of Northern China. *Environ. Sci. Pollut. Res.* 30, 85446–85465. <https://doi.org/10.1007/s11356-023-28333-y>.
- Angert, A., Cappa, C.D., DePaolo, D.J., 2004. Kinetic <sup>170</sup>O effects in the hydrologic cycle: Indirect evidence and implications. *Geochim. Et Cosmochim. Acta* 68, 3487–3495. <https://doi.org/10.1016/j.gca.2004.02.010>.
- Asano, Y., Uchida, T., 2018. The roles of channels and hillslopes in rainfall/run-off lag times during intense storms in a steep catchment. *Hydrol. Process.* 32, 713–728. <https://doi.org/10.1002/hyp.11443>.
- Baldwin, A.K., Corsi, S.R., Mason, S.A., 2016. Plastic Debris in 29 great lakes tributaries: relations to watershed attributes and hydrology. *Environ. Sci. Technol.* 50, 10377–10385. <https://doi.org/10.1021/acs.est.6b02917>.
- Broxton, D.E., Vaniman, D.T., 2005. Geologic framework of a groundwater system on the margin of a rift basin, Pajarito Plateau, north-central New Mexico. *Vadose Zone J.* 4, 522–550. <https://doi.org/10.2136/vzj2004.0073>.
- Cameira, M.D., Rolim, J., Valente, F., Mesquita, M., Dragosits, U., Cordovil, C., 2021. Translating the agricultural N surplus hazard into groundwater pollution risk: Implications for effectiveness of mitigation measures in nitrate vulnerable zones. *Agric. Ecosyst. Environ.* 306. <https://doi.org/10.1016/j.agee.2020.107204>.
- Chen, G.X., Li, G., Liang, A.M., Dong, Z.B., Liu, X.K., Ma, F., Cao, M., Yu, J.L., Sadiq, M., 2024a. Fingerprinting aeolian sediment sources in the Mu Us Sandy Land using the MixSIAR model. *Catena* 241. <https://doi.org/10.1016/j.catena.2024.108049>.
- Chen, S.H., Zhang, S.W., Hu, T.T., Li, H., Sun, J.X., Sun, G.Z., Liu, J., 2024b. Responses of soil reactive nitrogen pools and enzyme activities to water and nitrogen levels and their relationship with apple yield and quality under drip fertigation. *Sci. Hortic.* 324. <https://doi.org/10.1016/j.scienta.2023.112632>.
- Chittolina, M., da Rocha, H.R., Domingues, L.M., Lobo, G., 2023. Hydrological response of a headwater catchment in Southeast Brazil: Threshold patterns of stormflow response. *Hydrol. Process.* 37. <https://doi.org/10.1002/hyp.14879>.
- Craig, H., 1961. Isotopic Variations in Meteoric Waters. *Science* 133, 1702–1703. <https://doi.org/10.1126/science.133.3465.1702>.
- Dodds, W.K., Smith, V.H., 2016. Nitrogen, phosphorus, and eutrophication in streams. *Inland Waters* 6, 155–164. <https://doi.org/10.5268/iw.6.2.909>.
- El Mountassir, O., Bahir, M., Ouazar, D., Chehbouni, A., Carreira, P.M., 2022. Temporal and spatial assessment of groundwater contamination with nitrate using nitrate pollution index (NPI), groundwater pollution index (GPI), and GIS (case study: Essaouira basin, Morocco). *Environ. Sci. Pollut. Res.* 29, 17132–17149. <https://doi.org/10.1007/s11356-021-16922-8>.
- Ezzati, G., Kyllmar, K., Barron, J., 2023. Long-term water quality monitoring in agricultural catchments in Sweden: Impact of climatic drivers on diffuse nutrient loads. *Sci. Total Environ.* 864, 160978. <https://doi.org/10.1016/j.scitotenv.2022.160978>.
- Fatichi, S., Vivoni, E.R., Ogden, F.L., Ivanov, V.Y., Mirus, B., Gochis, D., Downer, C.W., Camporese, M., Davison, J.H., Ebel, B.A., Jones, N., Kim, J., Mascaro, G., Niswonger, R., Restrepo, P., Rigon, R., Shen, C., Sulis, M., Tarboton, D., 2016. An overview of current applications, challenges, and future trends in distributed process-based models in hydrology. *J. Hydrol.* 537, 45–60. <https://doi.org/10.1016/j.jhydrol.2016.03.026>.
- Fu, Y.F., Si, L.Y., Jin, Y., Xia, Z.Q., Wang, Q., Lu, H.D., 2022. Efficacy of black plastic film mulching as a cultivation strategy to cope with leaf senescence and increase yield of rainfed spring maize (*Zea mays* L.). *Soil Use Manag.* 38, 1044–1053. <https://doi.org/10.1111/sum.12677>.
- Fuentes-Rivas, R.M., Martínez-Alva, G., Ramos-Leal, J.A., de León, G.S., Moran-Ramírez, J., de Oca, R., 2020. Assessment of contamination by anthropogenic dissolved organic matter in the aquifer that underlies the agricultural area. *Environ. Sci. Pollut. Res.* 27, 45859–45873. <https://doi.org/10.1007/s11356-020-10512-w>.
- Gao, H.B., Wang, G., Fan, Y.R., Wu, J.F., Yao, M.Y., Zhu, X.F., Guo, X., Long, B., Zhao, J., 2024. Tracing groundwater nitrate sources in an intensive agricultural region integrated of a self-organizing map and end-member mixing model tool. *Sci. Rep.* 14. <https://doi.org/10.1038/s41598-024-67735-x>.
- Gao, J.B., Li, Z.Q., Chen, Z.J., Zhou, Y., Liu, W.G., Wang, L., Zhou, J.B., 2021a. Deterioration of groundwater quality along an increasing intensive land use pattern in a small catchment. *Agric. Water Manag.* 253. <https://doi.org/10.1016/j.agwat.2021.106953>.
- Gao, J.B., Wang, S.M., Li, Z.Q., Wang, L., Chen, Z.J., Zhou, J.B., 2021c. High nitrate accumulation in the vadose zone after land-use change from croplands to orchards. *Environ. Sci. Technol.* 55, 5782–5790. <https://doi.org/10.1021/acs.est.0c06730>.
- Gao, J.B., Li, Z.Q., Chen, Z.J., Zhou, Y., Liu, W.G., Wang, L., Zhou, J.B., 2021b. Deterioration of groundwater quality along an increasing intensive land use pattern in a small catchment. *Agric. Water Manag.* 253, 106953. <https://doi.org/10.1016/j.agwat.2021.106953>.
- Gao, X.D., Zhao, X.N., Wu, P.T., Yang, M., Ye, M.T., Tian, L., Zou, Y.F., Wu, Y., Zhang, F. S., Siddique, K.H.M., 2021d. The economicenvironmental trade-off of growing apple trees in the drylands of China: a conceptual framework for sustainable intensification. *J. Clean. Prod.* 296, 126497. <https://doi.org/10.1016/j.jclepro.2021.126497>.
- Hamidi, M.D., Gröcke, D.R., Joshi, S.K., Greenwell, H.C., 2023a. Investigating groundwater recharge using hydrogen and oxygen stable isotopes in Kabul city, a semi-arid region. *J. Hydrol.* 626. <https://doi.org/10.1016/j.jhydrol.2023.130187>.
- Hamidi, M.D., Gröcke, D.R., Joshi, S.K., Greenwell, H.C., 2023b. Investigating groundwater recharge using hydrogen and oxygen stable isotopes in Kabul city, a semi-arid region. *J. Hydrol.* 626, 130187. <https://doi.org/10.1016/j.jhydrol.2023.130187>.
- He, S.J., Lu, J., 2016. Contribution of baseflow nitrate export to non-point source pollution. *Sci. China-Earth Sci.* 59, 1912–1929. <https://doi.org/10.1007/s11430-016-5329-1>.
- He, Y.J., Wang, Y.Y., Liu, Y., Peng, B.R., Wang, G.L., 2024. Focus on the nonlinear infiltration process in deep vadose zone. *Earth-Sci. Rev.* 252. <https://doi.org/10.1016/j.earscirev.2024.104719>.
- He, Z.K., Han, D.M., Song, X.F., Yang, S.T., 2020. Impact of human activities on coastal groundwater pollution in the Yang-Dai River plain, northern China. *Environ. Sci. Pollut. Res.* 27, 37592–37613. <https://doi.org/10.1007/s11356-020-09760-7>.
- Hou, L.Z., Fan, X.J., Qi, Z.M., Wan, L., Hu, K.L., 2023. Simulation of water drainage and nitrate leaching at an irrigated maize (*Zea mays* L.) oasis cropland with a shallow groundwater table. *Agric. Ecosyst. Environ.* 355. <https://doi.org/10.1016/j.agee.2023.108573>.
- Hu, M.P., Liu, Y.M., Zhang, Y.F., Dahlgren, R.A., Chen, D.J., 2019. Coupling stable isotopes and water chemistry to assess the role of hydrological and biogeochemical processes on riverine nitrogen sources. *Water Res.* 150, 418–430. <https://doi.org/10.1016/j.watres.2018.11.082>.
- Hu, M.P., Zhang, Y.F., Wu, K.B., Shen, H., Yao, M.Y., Dahlgren, R.A., Chen, D.J., 2020. Assessment of streamflow components and hydrologic transit times using stable isotopes of oxygen and hydrogen in waters of a subtropical watershed in eastern China. *J. Hydrol.* 589. <https://doi.org/10.1016/j.jhydrol.2020.125363>.
- Huang, T.M., Ma, B.Q., Pang, Z.H., Li, Z., Li, Z.B., Long, Y., 2020. How does precipitation recharge groundwater in loess aquifers? Evidence from multiple environmental tracers. *J. Hydrol.* 583. <https://doi.org/10.1016/j.jhydrol.2019.124532>.
- Huang, Y.A., Li, B.A., Li, Z., 2021. Conversion of degraded farmlands to orchards decreases groundwater recharge rates and nitrate gains in the thick loess deposits. *Agric. Ecosyst. Environ.* 314, 107410. <https://doi.org/10.1016/j.agee.2021.107410>.
- Ji, X., Xie, R., Hao, Y., Lu, J., 2017. Quantitative identification of nitrate pollution sources and uncertainty analysis based on dual isotope approach in an agricultural watershed. *Environ. Pollut.* 229, 586–594. <https://doi.org/10.1016/j.envpol.2017.06.100>.
- Jiao, P.J., Xu, D., Wang, S.L., Yu, Y.D., Han, S.J., 2015. Improved SCS-CN method based on storage and depletion of antecedent daily precipitation. *Water Resour. Manag.* 29, 4753–4765. <https://doi.org/10.1007/s11269-015-1088-6>.
- Ju, Y.J., Koh, D.C., Kim, D.H., Mayer, B., Kwon, H.I., 2023. Evaluating the sources and fate of nitrate in riparian aquifers under agricultural land using in situ-measured noble gases, stable isotopes, and metabolic genes. *Water Res.* 231. <https://doi.org/10.1016/j.watres.2023.119601>.
- Juez, C., Garijo, N., Nadal-Romero, E., Vicente-Serrano, S.M., 2022. Wavelet analysis of hydro-climatic time-series and vegetation trends of the Upper Arag acute accent on catchment (Central Spanish Pyrenees). *J. Hydrol.* 614. <https://doi.org/10.1016/j.jhydrol.2022.128584>.
- Kaown, D., Koh, D.C., Mayer, B., Mahlknecht, J., Ju, Y.J., Rhee, S.K., Kim, J.H., Park, D. K., Park, I., Lee, H.L., Yoon, Y.Y., Lee, K.K., 2023b. Estimation of nutrient sources and fate in groundwater near a large weir-regulated river using multiple isotopes and microbial signatures. *J. Hazard. Mater.* 446. <https://doi.org/10.1016/j.jhazmat.2022.130703>.
- Kaown, D., Koh, D.C., Mayer, B., Mahlknecht, J., Ju, Y.J., Rhee, S.K., Kim, J.H., Park, D. K., Park, I., Lee, H.L., Yoon, Y.Y., Lee, K.K., 2023a. Estimation of nutrient sources and fate in groundwater near a large weir-regulated river using multiple isotopes and microbial signatures. *J. Hazard. Mater.* 446, 130703. <https://doi.org/10.1016/j.jhazmat.2022.130703>.
- Kataoka, T., Nihei, Y., Kudou, K., Hinata, H., 2019. Assessment of the sources and inflow processes of microplastics in the river environments of Japan. *Environ. Pollut.* 244, 958–965. <https://doi.org/10.1016/j.envpol.2018.10.111>.
- Li, T.J., Wang, G.Q., Huang, Y.F., Fu, X.D., 2009. Modeling the process of hillslope soil erosion in the loess plateau. *J. Environ. Inform.* 14, 1–10. <https://doi.org/10.3808/jei.200900148>.

- Li, X.Q., Li, S.Q., Qiang, X.L., Yu, Z., Sun, Z.J., Wang, R., He, J., Han, L., Li, Q., 2024. Effects of water and nitrogen regulation on apple tree growth, yield, quality, and their water and nitrogen utilization efficiency. *Plants-Basel* 13. <https://doi.org/10.3390/plants13172404>.
- Li, Z.J., Li, Z.X., Qi, F., Liu, X.Y., Gui, J., Xue, J., 2023. Quantitative analysis of recharge sources of different runoff types in the source region of Three River. *J. Hydrol.* 626. <https://doi.org/10.1016/j.jhydrol.2023.130366>.
- Liang, T., Tong, Y., Liu, X., Xu, W., Luo, X., Christie, P., 2016. High nitrogen deposition in an agricultural ecosystem of Shaanxi, China. *Environ. Sci. Pollut. Res. Int.* 23, 13210–13221. <https://doi.org/10.1007/s11356-016-6374-1>.
- Libutti, A., Monteleone, M., 2017. Soil vs. groundwater: The quality dilemma. Managing nitrogen leaching and salinity control under irrigated agriculture in Mediterranean conditions. *Agric. Water Manag.* 186, 40–50. <https://doi.org/10.1016/j.agwat.2017.02.019>.
- Liu, J.L., Zhan, A., Bu, L.D., Zhu, L., Luo, S.S., Chen, X.P., Cui, Z.L., Li, S.Q., Hill, R.L., Zhao, Y., 2014. Understanding dry matter and nitrogen accumulation for high-yielding film-mulched maize. *Agron. J.* 106, 390–396. <https://doi.org/10.2134/agronj2013.0404>.
- Liu, Y.Q., Zhang, X., Wu, Q.Y., 2018. Effects of landscape pattern change on non-point source pollution in coastal zone. *J. Coast. Res.* 756–760. <https://doi.org/10.2112/si85-152.1>.
- Lv, Y., Gao, L., Geris, J., Verrot, L., Peng, X., 2018. Assessment of water sources and their contributions to streamflow by end-member mixing analysis in a subtropical mixed agricultural catchment. *Agric. Water Manag.* 203, 411–422, 10.1016/j.agwat.2018.03.013.
- Lyu, S.X., Zhai, Y.Y., Zhang, Y.Q., Cheng, L., Paul, P.K., Song, J.X., Wang, Y.T., Huang, M. D., Fang, H.Y., Zhang, J.L., 2022. Baseflow signature behaviour of mountainous catchments around the North China Plain. *J. Hydrol.* 606. <https://doi.org/10.1016/j.jhydrol.2022.127450>.
- Matsuizaki, Y., Kubota, M., 2024. Uncertainty in river discharge forcings and error range on nowcasting numerical simulation of salinity and seawater temperature in Ise Bay, Japan. *Mar. Pollut. Bull.* 207, 116734, 10.1016/j.marpolbul.2024.116734.
- Miao, P., Zhu, X.Q., Zhang, S.F., Li, W.H., Zhou, J.B., Chen, Z.J., 2023. Long-term high nitrogen surplus in intensive apple-planting regions results in huge legacy nitrogen in the vadose zone: Potential or real risk to the groundwater? *Agric. Ecosyst. Environ.* 357. <https://doi.org/10.1016/j.agee.2023.108682>.
- Miao, P., Zhu, X.Q., Zhang, S.F., Li, W.H., Zhou, J.B., Chen, Z.J., 2023. Long-term high nitrogen surplus in intensive apple-planting regions results in huge legacy nitrogen in the vadose zone: Potential or real risk to the groundwater? *Agric. Ecosyst. Environ.* 357. <https://doi.org/10.1016/j.agee.2023.108682>.
- Mihiranga, H.K.M., Jiang, Y., Sathsarani, M.G.S., Li, X.Y., Ritigala, T., Demissie, H.L., Wang, W., 2022. Identification of rainy season nitrogen export controls in a semi-arid mountainous watershed, North China. *Sci. Total Environ.* 839. <https://doi.org/10.1016/j.scitotenv.2022.156293>.
- Mo, X.Y., Peng, H., Xin, J., Wang, S., 2022. Analysis of urea nitrogen leaching under high-intensity rainfall using HYDRUS-1D. *J. Environ. Manag.* 312. <https://doi.org/10.1016/j.jenvman.2022.114900>.
- Nan, W.G., Yue, S.C., Li, S.Q., Huang, H.Z., Shen, Y.F., 2016. Characteristics of N<sub>2</sub>O production and transport within soil profiles subjected to different nitrogen application rates in China. *Sci. Total Environ.* 542, 864–875. <https://doi.org/10.1016/j.scitotenv.2015.10.147>.
- Niu, X.Q., Jia, X.X., Yang, X.F., Wang, J., Wei, X.R., Wu, L.H., Shao, M.G., 2022. Tracing the sources and fate of NO<sub>3</sub><sup>-</sup> in the vadose zone - groundwater system of a thousand-year-cultivated region. *Environ. Sci. Technol.* 56, 9335–9345. <https://doi.org/10.1021/acs.est.1c06289>.
- Ongley, E.D., Zhang, X.L., Yu, T., 2010. Current status of agricultural and rural non-point source Pollution assessment in China. *Environ. Pollut.* 158, 1159–1168. <https://doi.org/10.1016/j.envpol.2009.10.047>.
- Park, J.Y., Ruudisch, M., Huwe, B., 2016. Transport of sulfonamide antibiotics in crop fields during monsoon season. *Environ. Sci. Pollut. Res.* 23, 22980–22992. <https://doi.org/10.1007/s11356-016-7465-8>.
- Qin, B.Q., Zhang, Y.L., Zhu, G.W., Gao, G., 2023. Eutrophication control of large shallow lakes in China. *Sci. Total Environ.* 881. <https://doi.org/10.1016/j.scitotenv.2023.163494>.
- Ren, K., Pan, X.D., Yuan, D.X., Zeng, J., Liang, J.P., Peng, C., 2022. Nitrate sources and nitrogen dynamics in a karst aquifer with mixed nitrogen inputs (Southwest China): revealed by multiple stable isotopic and hydro-chemical proxies. *Water Res.* 210. <https://doi.org/10.1016/j.watres.2021.118000>.
- Ren, M., Li, C.J., Gao, X.D., Niu, H.H., Cai, Y.H., Wen, H.X., Yang, M.H., Siddique, K.H. M., Zhao, X.N., 2023. High nutrients surplus led to deep soil nitrate accumulation and acidification after cropland conversion to apple orchards on the Loess Plateau, China. *Agric. Ecosyst. Environ.* 351. <https://doi.org/10.1016/j.agee.2023.108482>.
- Robinson, B.A., Cole, G., Carey, J.W., Witkowski, M., Gable, C.W., Lu, Z.M., Gray, R., 2005. A vadose zone flow and transport model for Los Alamos Canyon, Los Alamos, New Mexico. *Vadose Zone J.* 4, 729–743. <https://doi.org/10.2136/vzj2004.0169>.
- Samantara, M.K., Padhi, R.K., Satpathy, K.K., Sowmya, M., Kumaran, P., 2015. Groundwater nitrate contamination and use of Cl/Br ratio for source appointment. *Environ. Monit. Assess.* 187. <https://doi.org/10.1007/s10661-014-4211-x>.
- Schulte-Uebbing, L.F., Beusen, A.H.W., Bouwman, A.F., de Vries, W., 2022. From planetary to regional boundaries for agricultural nitrogen pollution. *Nature* 610, 507. <https://doi.org/10.1038/s41586-022-05158-2>.
- Serra, J., Cameira, M.D., Cordovil, C., Hutchings, N.J., 2021. Development of a groundwater contamination index based on the agricultural hazard and aquifer vulnerability: application to Portugal. *Sci. Total Environ.* 772. <https://doi.org/10.1016/j.scitotenv.2021.145032>.
- Shang, X., Huang, H., Mei, K., Xia, F., Chen, Z., Yang, Y., Dahlgren, R.A., Zhang, M., Ji, X., 2020. Riverine nitrate source apportionment using dual stable isotopes in a drinking water source watershed of southeast China. *Sci. Total Environ.* 724, 137975, 10.1016/j.scitotenv.2020.137975.
- Shen, W.C., Zhang, J.J., Wang, K., Zhang, Z.F., 2023. Identifying the spatio-temporal dynamics of regional ecological risk based on Google Earth Engine: a case study from Loess Plateau, China. *Sci. Total Environ.* 873. <https://doi.org/10.1016/j.scitotenv.2023.162346>.
- Shukla, S., Saxena, A., 2020. Sources and leaching of nitrate contamination in groundwater. *Curr. Sci.* 118, 883–891. <https://doi.org/10.18520/cs/v118/i6/883-891>.
- Song, X.L., Wu, P.T., Gao, X.D., Yao, J., Zou, Y.F., Zhao, X.N., Siddique, K.H.M., Hu, W., 2020. Rainwater collection and infiltration (RWCI) systems promote deep soil water and organic carbon restoration in water-limited sloping orchards. *Agric. Water Manag.* 242, 106400. <https://doi.org/10.1016/j.agwat.2020.106400>.
- Stock, B.C., Jackson, A.L., Ward, E.J., Parnell, A.C., Phillips, D.L., Semmens, B.X., 2018. Analyzing mixing systems using a new generation of Bayesian tracer mixing models. *PeerJ* 6. <https://doi.org/10.7717/peerj.5096>.
- Sun, H.P., Zheng, W.B., Wang, S.Q., Ma, L., Min, L.L., Shen, Y.J., 2024. Variation of nitrate sources affected by precipitation with different intensities in groundwater in the piedmont plain area of alluvial-pluvial fan. *J. Environ. Manag.* 367. <https://doi.org/10.1016/j.jenvman.2024.121885>.
- Tillman, F.D., Gangopadhyay, S., Pruitt, T., 2016. Changes in groundwater recharge under projected climate in the upper Colorado River basin. *Geophys. Res. Lett.* 43, 6968–6974. <https://doi.org/10.1002/2016gl069714>.
- Torres-Martinez, J.A., Mora, A., Knappett, P.S.K., Ornelas-Soto, N., Mahlknecht, J., 2020. Tracking nitrate and sulfate sources in groundwater of an urbanized valley using a multi-tracer approach combined with a Bayesian isotope mixing model. *Water Res.* 182. <https://doi.org/10.1016/j.watres.2020.115962>.
- Torres-Martinez, J.A., Mora, A., Mahlknecht, J., Daesslé, L.W., Cervantes-Avilés, P.A., Ledesma-Ruiz, R., 2021. Estimation of nitrate pollution sources and transformations in groundwater of an intensive livestock-agricultural area (Comarca Lagunera), combining major ions, stable isotopes and MixSIAR model. *Environ. Pollut.* 269, 115445. <https://doi.org/10.1016/j.envpol.2020.115445>.
- Turkeltaub, T., Jia, X.X., Zhu, Y.J., Shao, M.A., Binley, A., 2021. A comparative study of conceptual model complexity to describe water flow and nitrate transport in deep unsaturated loess. *Water Resour. Res.* 57. <https://doi.org/10.1029/2020wr029250>.
- Wang, D., Li, P.Y., Yang, N.N., Yang, C.L., Zhou, Y.H., Li, J.H., 2023. Distribution, sources and main controlling factors of nitrate in a typical intensive agricultural region, northwestern China: vertical profile perspectives. *Environ. Res.* 237. <https://doi.org/10.1016/j.envres.2023.116911>.
- Wang, J., Li, X., Li, Y., Shi, Y.Y., Xiao, H.B., Wang, L., Yin, W., Zhu, Z.Y., Bian, H.X., Li, H., Y., Shi, Z.H., Seybold, H., Kirchner, J.W., 2024. Transport pathways of nitrate in stormwater runoff inferred from high-frequency sampling and stable water isotopes. *Environ. Sci. Technol.* 58, 17026–17035. <https://doi.org/10.1021/acs.est.4c02495>.
- Wang, W.Y., Yuan, J.C., Gao, S.M., Li, T., Li, Y.J., Vinay, N., Mo, F., Liao, Y.C., Wen, X.X., 2020. Conservation tillage enhances crop productivity and decreases soil nitrogen losses in a rainfed agroecosystem of the Loess Plateau, China. *J. Clean. Prod.* 274. <https://doi.org/10.1016/j.jclepro.2020.122854>.
- Wang, Y.X., Liu, G.H., Zhao, Z.H., Wu, C.S., Yu, B.W., 2021. Using soil erosion to locate nonpoint source pollution risks in coastal zones: a case study in the Yellow River Delta, China. *Environ. Pollut.* 283, 117117. <https://doi.org/10.1016/j.envpol.2021.117117>.
- Wang, Y.X., Li, C.L., Qiao, J.M., Hu, Y.M., Zhang, Q., Yin, J.B., Slater, L., 2025. Meta-analysis of urban non-point source pollution from road and roof runoff across China. *Earth's Future* 13. <https://doi.org/10.1029/2024ef005296>.
- Wang, Z.J., Yue, F.J., Wang, Y.C., Qin, C.Q., Ding, H., Xue, L.L., Li, S.L., 2022. The effect of heavy rainfall events on nitrogen patterns in agricultural surface and underground streams and the implications for karst water quality protection. *Agric. Water Manag.* 266. <https://doi.org/10.1016/j.agwat.2022.107600>.
- Warrix, S.R., Navarre-Sitchler, A., Manning, A.H., Singha, K., 2023. Local topography and streambed hydraulic conductivity influence riparian groundwater age and groundwater-surface water connection. *Water Resour. Res.* 59. <https://doi.org/10.1029/2023wr035044>.
- Wei, M.Z., Liu, J.W., Yang, Q.Z., Xue, A., Wu, H., Ni, J.R., Winter, L.R., Elimelech, M., Zhao, H.Z., 2022. Denitrification mechanism in oxygen-rich aquatic environments through long-distance electron transfer. *Npj Clean Water* 5. <https://doi.org/10.1038/s41545-022-00205-x>.
- Wells, M.J., Gilmore, T.E., Nelson, N., Mittelstet, A., Böhlke, J.K., 2021. Determination of vadose zone and saturated zone nitrate lag times using long-term groundwater monitoring data and statistical machine learning. *Hydrog. Earth Syst. Sci.* 25, 811–829. <https://doi.org/10.5194/hess-25-811-2021>.
- Xiao, Q.T., Hu, Z.H., Fu, C.S., Bian, H., Lee, X.H., Chen, S.T., Shang, D.Y., 2019. Surface nitrous oxide concentrations and fluxes from water bodies of the agricultural watershed in Eastern China. *Environ. Pollut.* 251, 185–192. <https://doi.org/10.1016/j.envpol.2019.04.076>.
- Xiao, Q.T., Xu, X.F., Duan, H.T., Qi, T.C., Qin, B.Q., Lee, X., Hu, Z.H., Wang, W., Xiao, W., Zhang, M., 2020. Eutrophic Lake Taihu as a significant CO<sub>2</sub> source during 2000–2015. *Water Res.* 170. <https://doi.org/10.1016/j.watres.2019.115331>.
- Xiao, X., Zhang, X.P., Wu, H.W., Zhang, C.C., Han, L.F., 2022. Stable isotopes of surface water and groundwater in a typical subtropical basin in south-central China: insights into the young water fraction and its seasonal origin. *Hydrol. Process.* 36. <https://doi.org/10.1002/hyp.14574>.
- Xie, H., Gao, T.T., Wan, N.S., Xiong, Z.Y., Dong, J.W., Lin, C., Lai, X.J., 2022. Controls for multi-temporal patterns of riverine nitrogen and phosphorus export to lake:

- implications for catchment management by high-frequency observations. *J. Environ. Manag.* 320. <https://doi.org/10.1016/j.jenvman.2022.115858>.
- Xu, W., Cai, Y.P., Rong, Q.Q., Yang, Z.F., Li, C.H., Wang, X., 2018. Agricultural non-point source pollution management in a reservoir watershed based on ecological network analysis of soil nitrogen cycling. *Environ. Sci. Pollut. Res.* 25, 9071–9084. <https://doi.org/10.1007/s11356-017-1092-x>.
- Xue, D.M., Botte, J., De Baets, B., Accoe, F., Nestler, A., Taylor, P., Van Cleemput, O., Berglund, M., Boeckx, P., 2009. Present limitations and future prospects of stable isotope methods for nitrate source identification in surface- and groundwater. *Water Res.* 43, 1159–1170. <https://doi.org/10.1016/j.watres.2008.12.048>.
- Yan, Y.J., Yang, Y.Q., Dai, Q.H., 2023. Effects of preferential flow on soil nutrient transport in karst slopes after recultivation. *Environ. Res. Lett.* 18. <https://doi.org/10.1088/1748-9326/acb8c>.
- Yao, P.W., Li, X.S., Nan, W.G., Li, X.Y., Zhang, H.P., Shen, Y.F., Li, S.Q., Yue, S.C., 2017. Carbon dioxide fluxes in soil profiles as affected by maize phenology and nitrogen fertilization in the semiarid Loess Plateau. *Agric. Ecosyst. Environ.* 236, 120–133. <https://doi.org/10.1016/j.agee.2016.11.020>.
- Yu, Y.L., Jin, Z., Chu, G.C., Zhang, J., Wang, Y.Q., Zhao, Y.L., 2020. Effects of valley reshaping and damming on surface and groundwater nitrate on the Chinese Loess Plateau. *J. Hydrol.* 584. <https://doi.org/10.1016/j.jhydrol.2020.124702>.
- Zhai, X.Y., Guo, L., Liu, R.H., Zhang, Y.Y., Zhang, Y.Q., 2021. Comparing three hydrological models for flash flood simulations in 13 humid and semi-humid mountainous catchments. *Water Resour. Manag.* 35, 1547–1571. <https://doi.org/10.1007/s11269-021-02801-x>.
- Zhang, C.Y., Zhang, S., Yin, M.Y., Ma, L.N., He, Z., Ning, Z., 2013. Nitrogen isotope studies of nitrate contamination of the thick vadose zones in the wastewater-irrigated area. *Environ. Earth Sci.* 68, 1475–1483. <https://doi.org/10.1007/s12665-012-1878-6>.
- Zhang, W., Li, S.Q., Shen, Y.F., Yue, S.C., 2021a. Film mulching affects root growth and function in dryland maize-soybean intercropping. *Field Crops Res.* 271. <https://doi.org/10.1016/j.fcr.2021.108240>.
- Zhang, X., Zhang, Y., Shi, P., Bi, Z.L., Shan, Z.X., Ren, L.J., 2021b. The deep challenge of nitrate pollution in river water of China. *Sci. Total Environ.* 770, 144674. <https://doi.org/10.1016/j.scitotenv.2020.144674>.
- Zhou, P., Bai, X.L., Wang, H.Y., Yang, M.X., Bao, L., Deng, X.F., Chen, Z.J., Zhou, J.B., 2023. Optimizing nitrogen and water management for sustainable greenhouse vegetable production with less greenhouse gas emissions. *Agric. Ecosyst. Environ.* 352. <https://doi.org/10.1016/j.agee.2023.108529>.
- Zhu, X.Q., Fu, W.H., Kong, X.J., Chen, C.X., Liu, Z.J., Chen, Z.J., Zhou, J.B., 2021. Nitrate accumulation in the soil profile is the main fate of surplus nitrogen after land-use change from cereal cultivation to apple orchards on the Loess Plateau. *Agric. Ecosyst. Environ.* 319, 107574. <https://doi.org/10.1016/j.agee.2021.107574>.
- Zhu, X.Q., Miao, P., Wang, P.Z., Zhang, S.F., Chen, Z.J., Zhou, J.B., 2022. Variations and influencing factors of nitrate accumulation in the deep soil profiles of apple orchards on the Loess Plateau. *Agric. Ecosyst. Environ.* 335, 108005. <https://doi.org/10.1016/j.agee.2022.108005>.
- Zhu, X.Q., Miao, P., Qin, J.M., Li, W.H., Wang, L., Chen, Z.J., Zhou, J.B., 2023. Spatio-temporal variations of nitrate pollution of groundwater in the intensive agricultural region: Hotspots and driving forces. *J. Hydrol.* 623, 129864. <https://doi.org/10.1016/j.jhydrol.2023.129864>.
- Zou, L.L., Liu, Y.S., Wang, Y.S., Hu, X.D., 2020. Assessment and analysis of agricultural non-point source pollution loads in China: 1978–2017. *J. Environ. Manag.* 263. <https://doi.org/10.1016/j.jenvman.2020.110400>.